RSC Advances

REVIEW

View Article Online
View Journal | View Issue

Cite this: *RSC Adv.*, 2024, **14**, 9365

Design and application of metal organic frameworks for heavy metals adsorption in water: a review

S. Essalmi,[ab] S. Lotfi,[a] A. BaQais,[c] M. Saadi,[a] M. Arab[b] and H. Ait Ahsaine*[a]

The growing apprehension surrounding heavy metal pollution in both environmental and industrial contexts has spurred extensive research into adsorption materials aimed at efficient remediation. Among these materials, Metal–Organic Frameworks (MOFs) have risen as versatile and promising contenders due to their adjustable properties, expansive surface areas, and sustainable characteristics, compared to traditional options like activated carbon and zeolites. This exhaustive review delves into the synthesis techniques, structural diversity, and adsorption capabilities of MOFs for the effective removal of heavy metals. The article explores the evolution of MOF design and fabrication methods, highlighting pivotal parameters influencing their adsorption performance, such as pore size, surface area, and the presence of functional groups. In this perspective review, a thorough analysis of various MOFs is presented, emphasizing the crucial role of ligands and metal nodes in adapting MOF properties for heavy metal removal. Moreover, the review delves into recent advancements in MOF-based composites and hybrid materials, shedding light on their heightened adsorption capacities, recyclability, and potential for regeneration. Challenges for optimization, regeneration efficiency and minimizing costs for large-scale applications are discussed.

Received 24th December 2023
Accepted 7th March 2024

DOI: 10.1039/d3ra08815d

rsc.li/rsc-advances

1. Introduction

Environmental degradation refers to the deterioration of the natural environment, including the air, water, and land.[1] There are a variety of causes of environmental degradation, including human activities like deforestation, mining, and the use of fossil fuels for energy production. These activities release pollutants into the air and water, leading to air and water pollution. Additionally, overfishing, climate change, and the destruction of habitats through urbanization all play a role in environmental degradation. Addressing these issues requires concerted efforts to reduce pollution, protect habitats, and move towards more sustainable practices for energy production and resource use. Industrialization often leads to polluted water. This is because many industrial processes use chemicals and produce waste that can contaminate water sources. Additionally, industrial facilities may discharge wastewater containing organic and inorganic pollutants into rivers.[2,3] These pollutants can affect humans and wildlife, as well as damage ecosystems. To address this issue, it is important to regulate industrial practices and ensure that they are using best management practices to minimize their impact on the environment. It is also important to invest in technologies and systems that can help reduce pollution and treat wastewater before it is released into the environment.[4–12] Heavy metals are a common inorganic pollutant found in contaminated water sources. These metals can be harmful to human health and wildlife, so it is important to reduce their concentration in polluted water.[13–16]

Several techniques can be used to decrease concentration of heavy metals in polluted water like chemical precipitation, ion exchange, membrane filtration, adsorption, and electrochemical treatment. Table 1 summarized the main advantages and disadvantages of each method.[17–20]

It is important to select the right treatment method based on the type and concentration of heavy metals displayed in the polluted water. Additionally, regular testing and monitoring should be conducted to ensure the effectiveness of the chosen treatment method.[21] One common and interesting method is adsorption, which involves using materials such as activated carbon, zeolites, or biochar to attract and remove heavy metals from the water. There have been recent advancements in the range of adsorption for heavy metal elimination from water sources.[22] One such advancement is the use of nanomaterials as adsorbents, which have high surface area and high reactivity, allowing for more efficient elimination of heavy metals from water. Another advancement is the use of magnetic adsorbents, which can be effortlessly eliminated from the water using a magnetic field, making the process more efficient and cost-

[a]*Laboratoire de Chimie Appliquée des Matériaux, Centre des Sciences des Matériaux, Faculty of Sciences, MohammedV University in Rabat, Morocco. E-mail: h.aitahsaine@um5r.ac.ma*

[b]*Université de Toulon, AMU, CNRS, IM2NP, CS 60584, Toulon Cedex 9, France*

[c]*Department of Chemistry, College of Science, Princess Nourah Bint Abdulrahman University, P. O. Box 84428, Riyadh 11671, Saudi Arabia*

Table 1 Frequently used techniques for water treatment

Method	Advantages	Disadvantages
Chemical precipitation	Cost-effective Simple operation	Limited selectivity Chemical dependence
Ion exchange	High selectivity Reusable media	Sensitivity to competing ions High upfront cost
Membrane filtration	Highly effective Modular design	High energy consumption Limited applicability
Adsorption	Simple design Regenerable media	Limited capacity
Electrochemical treatment	Potential for automation	High energy consumption Electrode maintenance

effective.[23] Additionally, researchers are exploring the use of bio-based adsorbents, which utilize natural materials such as agricultural waste and plant fibers to remove heavy metals from water.[24] Recently several natural materials have been developed showing economic and environmental interest including horn snail, mangrove crab shell powder, bagasse–bentonite, *Archontophoenix alexandrae*, silica@mercapto, Bali cow bones-based hydrochar and microalgae for example *Chlorella vulgaris*.[25–34] These advancements show great promise in the field of heavy metal removal and offer hope for cleaner water sources in the future and can be combined with other more stable materials for water treatment.

MOFs or metal–organic frameworks have been studied for their potential to adsorb heavy metals from water. These microporous materials have high surface areas and may be adapting to selectively eliminate specific toxic elements. However, withal research is needed to optimize MOFs for practical applications and ensure their safety and environmental impact. Nonetheless, MOFs hold promise as a viable option for heavy metal removal in the future.[35]

The purpose of this overview is to discuss the syntheses approaches of MOFs based adsorbents from a predesigned materials perspective and to oversee the potential of MOFs-based porous materials in the elimination of heavy metals from contaminated water, then, limitations, future challenges and prospects are given to guide researchers for better adsorption-by-design approach.

2. Synthesis methods to produce MOFs

There are several methods that have been used to produce MOFs such as solvothermal and sonochemical methods, slow diffusion of trimethylamine (TEA) and mechanochemistry, *etc.* Fig. 1 presents the commonly used synthesis methods for the preparation of MOFs.

The researchers synthesized these MOFs using specific preparation methods referring to the percentage of use, as is shown in Fig. 2.

2.1. Solvothermal synthesis

The solvothermal method has been widely employed for the development of MOFs. This synthesis required the employee of

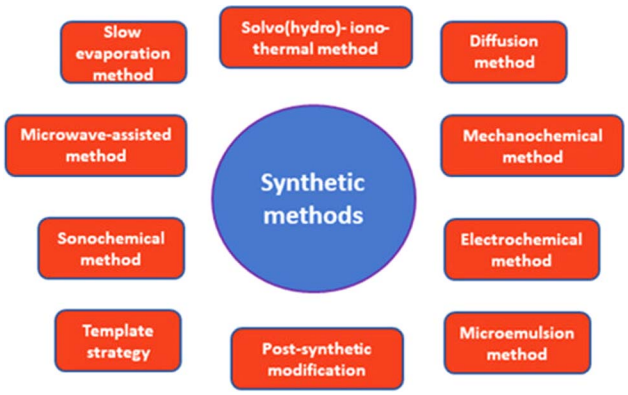

Fig. 1 Common synthesis approaches for MOFs. Reproduced with permission from ref. 36 Copyright © 2021, MDPI.

organic solvents with high solubilizing capability such as dimethylformamide (DMF), dimethylformamide (DEF), methanol, ethanol, and acetonitrile[38,39] the choice of solvents is crucial. McKinstry *et al.*[40] focused on production of MOF-5 by solvothermal process using two most common solvents *N*,*N*-diethylformamide (DEF) and *N*,*N* dimethylformamide (DMF) for comparison. They reported that the low temperature and slow time reactions lead to high surface areas.[41,42] In addition, Zhang *et al.*[43] prepared mesoporous/macroporous MOF nanosheets by facile solvothermal method using dimethylformamide (DMF) and methanol. They revealed that the obtained MOFs present different morphologies due to starting coordination complexes of different copper(II)-ligands, because they have an impact on size and shape. Also, they confirmed that the prepared MOFs nanosheets have a potential application with a high surface area, which can be explained by the involvement of mesoporous and macroporous cavities. Moreover, Kamal and co-workers[44] synthesized Nickel-based MOF-74 (Ni-MOF-74) by optimized solvothermal method using dimethylformamide (DMF) and methanol. They demonstrated that removing residual reactants like the reactive medium and the polluted methanol significantly improved CO_2 uptakes. Also, Nguyen *et al.*[45] developed microporous MOFs materials grounded on bismuth and trimesic acid (Bi-BTC) *via* solvothermal process[46] employing a mixture of dimethylformamide and methanol.[47] They evaluated the photocatalytic efficiency of the MOFs

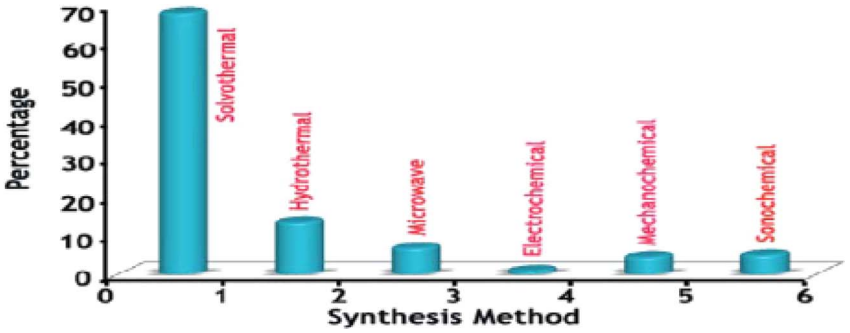

Fig. 2 The percentage of MOFs prepared by different methods. Reproduced with permission from ref. 37. Copyright © 2017, SciEP https://www.researchgate.net/journal/American-Journal-of-Environmental-Protection-2328-7241?_tp=eyJjb250ZXh0Ijp7ImZpcnN0UGFnZSI6InB1YmxpY2F0aW9uIiwicGFnZSI6InB1YmxpY2F0aW9uIiwicHJldmlvdXNQYWdlIjoiX2RpcmVjdCJ9fQ.

amongst photocatalytic decomposition of rhodamine B (RhB). As results, the mixing solvents had a good impact on the synthesis of porous rod-like morphologies of Bi-BTC with pore size of 1.7 nm and the largest specific surface area (148 $m^2 g^{-1}$). Therefore, solvents have influenced the morphology and structure. This material is characterized by optical bandgap value of 3.31 ev and RhB dye degradation efficiency of 95.06% after 100 min of light irradiation. However, solvothermal

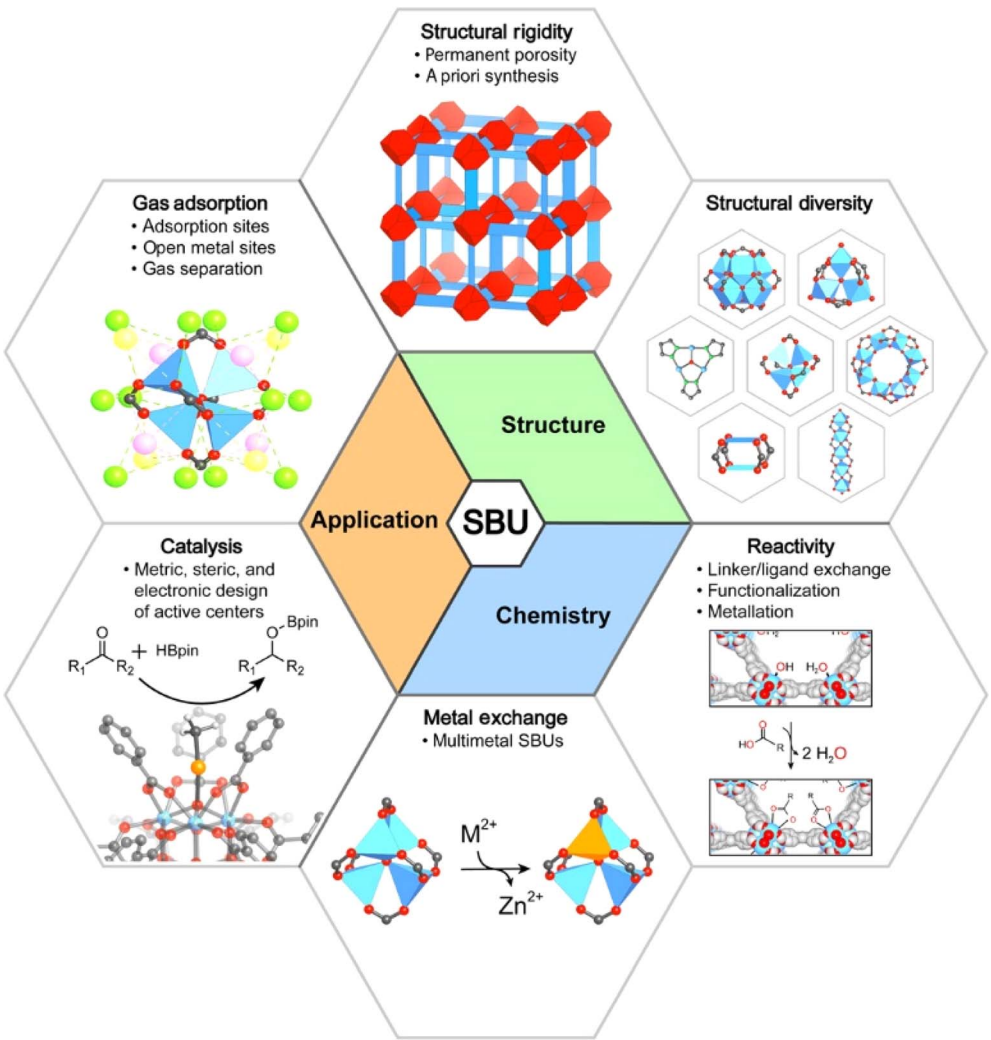

Fig. 3 Impact of the SBU on the structure, chemistry, and applications of MOFs. Reproduced with permission from ref. 92 Copyright © 2018, Wiley.

method have several limitations such as long reaction time, expensiveness and toxicity of solvents used which caused adverse health and environmental effects. Therefore, the researchers have developed a new solvent-free synthesis.

2.2. Slow diffusion of triethylamine (TEA)

This method has an influence on morphology, pore parameters and hydrogen storage capacity of MOF-5. According to Li *et al.* the slow diffusion of triethylamine (TEA) requires the presence of TEA and molar ratio of $Zn(NO_3)_2 \cdot 6H_2O/H_2BDC = 2/1$, DMF/$H_2BDC = 258.5/1$ for a reaction time of 48 h. MOF-5 have been synthesized with different degrees of crystallinity, small irregular shape, BET surface area of 481.1 $m^2 g^{-1}$ of and pore volume of 0.19 $cm^3 g^{-1}$. In a typical process, heat treatment 673 K and solvent extraction by chloroform would fully degrade the organic guests and generate a porous framework with hydrogen-storage capacity of 2.63 wt%.[48,49]

Gonte *et al.*[50] developed a Zn-BPDC MOFs incorporated in the pores of hyper crosslinked polymers beads by slow diffusion of TEA. They reported that the formation of Zn–polymer complex is assured between $Zn(NO_3)_2 \cdot 6H_2O$ and dicarboxylic acid. Therefore, the change of this dicarboxylic acid linker had a strong influence on the morphologies of the resultant MOFs that will decorate the pore surface of the polymers. Hu *et al.*[51] synthesized Zn_xMn_{1-x}MOF-74 nanoparticles *via* triethylamine (TEA) assistant solvothermal method. They prepared the Zn-MOF-74-*T* at different temperatures ($T = 25$, 45, 65, 85, 105 and 125 °C) using triethylamine (TEA), 2,5-dihydroxyterephthalic acid and dimethylformamide (DMF). Also, they prepared Zn_x-Mn_{1-x}-MOF-74 by following the same steps of Zn-MOF-74 synthesis just they replace the source of Zn by a mixture of $Zn(CH_3COO)_2 \cdot 2H_2O$ and $Mn(CH_3COO)_2 \cdot 4H_2O$.

The results revealed that the MOF-74 pure nanoparticles were successfully synthesized with different morphologies (plate-like and rod-like) and size particles with a marked influence of the high temperature on size. In addition, they show that the important amount of TEA lead to the formation of small crystallites that increased the peak broadenings and in the absence of TEA a rod-like shape was generated. Therefore, the presence of TEA and low temperature are necessary for the formation of Zn-MOF-74 porous nanoparticles. Finally, they have introduced the Mn^{2+} ions to prepare a bimetallic $Zn_{0.7}Mn_{0.3}$-MOF-74 nanoparticles of about 200 nm with rod-like shape and high surface area.

2.3. Sonochemical

The sonochemical method has been applied to produce elevated quality MOF-5 crystals of 5–25 μm for a reaction time of 30 min using high-intensity ultrasound to improve the reactivity of metals as a stoichiometric reagent. The sonochemistry is based on acoustic cavitation which involves the product, improvement, and destruction of a bubble in a liquid, which produces highly regional temperatures (5000–25 000 K) and pressures beside an extraordinary heating and cooling rate.[52,53] Son *et al.*[54] reported a sonochemical technique to synthesis MOF-5 cubic phase 155 °C with small size 5–25 μm. The reaction temperature was 155 °C for elevated quality S-MOF-5 crystals. This method assumes a surface area of 3208 $m^2 g^{-1}$ and a pore volume of 1.26 $cm^3 g^{-1}$, while the analogous values for C-MOF-5 were 3200 $m^2 g^{-1}$ and 1.21 $cm^3 g^{-1}$, properly. The thermal stability of the exemplification was tried exploiting a thermogravimetric analyzer (TGA, SCINCO Thermogravimeter S-1000): under air flow (30 mL min^{-1}), 10 mg of sample was heated to 700 °C. The results showed a weight loss at 430–470 °C and 1-methyl-2-pyrrolidone (NMP) as a suitable approach solvent for MOF-5. Saidi *et al.*[55] synthesized Zr-fumaric based metal–organic framework (MOF) under sonochemical conditions using fumaric acid, dimethylformamide DMF (40 mL) and formic acid. The prepared sample dried at two different temperatures (150 °C and 180 °C). They showed that at 180 °C the solvent molecules evaporate which frees the evaporation of solvent molecules which makes the pores free and displays high specific surface area. Therefore, the obtained sample provides a promising photocatalytic activity for degradation of organic dyes.

However, Wiwasuku *et al.*[56] reported synthesis of uniform octahedral Zn-MOF with smaller particles size by using sodium acetate as a modulator agent under 60 min of ultrasound irradiation at room temperature. Hwan Lee *et al.*[57] demonstrated a simple sonochemical method for preparing the MIL-53 (Fe) family of MOFs. The MIL-53(Fe) presented several properties: chemical stability, low toxicity, and simple synthesis.[58,59] In this method the researchers prepared the sample by UTS irradiation to reduce the grain size.[60,61] The results show that the sample obtained after 2 h of UTS irradiation exhibits a high crystallinity, open pore structure and particles with small size. In addition, Yu *et al.*[62] reported a synthesis of MOF-525 and MOF-545 by modulation[63,64] *via* a sonochemical method using a modulators benzoic acid for MOF-525, and trifluoroacetic acid for MOF-545. The modulators can induce local defect structures, control crystal purity, particle size and synthesis time.

2.4. Mechanochemistry

Mechanochemistry is based on grinding or ball milling. It is used for the synthesis of metal–organic frameworks at room temperature[65] and it is considered as an alternative green synthesis technique. The mechanochemistry has been demonstrated as an excellent technique which may be employed to reduce both the reaction time and solvents.[66] There are three main modes of mechanochemical reaction Neat Grinding (NG).[67–69] Liquid-assisted grinding (LAG)[70–72] and ion-and-liquid assisted grinding (ILAG) which is considered as the most efficient route to prepare MOFs thanks to the used of catalytic amounts of inorganic salts additives.[73–75] Julien *et al.*[76] have reported the mechanochemical synthesis of Zn-MOF-74 from ZnO and 2,5-dihydroxyterephthalic acid, using DMF as a liquid additive.

The process synthesis of Zn-MOF-74 can be explained by rapid reaction of acid groups on H_4dhta, leading to non-porous $Zn(H_2O)_2$ (H_2dhta), Which react with residual ZnO during grinding to have as result the Zn-MOF-74 product.

The results of the mechanosynthesis of Zn-MOF-74 by LAG with H_2O/DMF mixture revealed that these conditions lead to the formation of Zn-MOF-74 with high surface area.

Masoomi *et al.*[77] have developed two new 3D porous structure of MOFs, $(Cd_2(oba)_2(4\text{-bpdb})_2]_n$. (DMF)x (TMU-8) and $(Cd(oba)(4,4'\text{-bipy})]_n\cdot(DMF)_y$ (TMU-9) by mechanochemical milling *N*-donor ligands 1,4-bis(4-pyridyl)-2,3-diaza-1,3-butadiene (4-bpdb) and 4,4′-bipyridine (4,4′-bipy) and H_2oba. The results show that TMU-8 and TMU-9 have plate-like morphologies and larger pores. Wang *et al.*[78] developed a mechanochemical synthesis of MOF-74 by LAG, using liquid exogenous organic base Hünig's base (*N*,*N*-diisopropylethylamine) which assure the formation of the framework M_2(dobdc) analogues (M = Mg, Mn, Co, Ni, Cu, Zn; dobdc4– = 2,5-dioxidobenzene-1,4-dicarboxylate) and facilitate the grinding. This method is considered as a sustainable strategy because it needs short time reaction, ambient temperature and solvent-free conditions, in order to prepare nanocrystalline MOF-74 with smaller size and highly porous structure.

Recently, Beamish-Cook *et al.*[79] prepared MOF-74 by mechanochemical synthesis from ZnO and 2,5-dihydroxyterephthalic acid (H_4HDTA) using DMF as solvent.

They revealed that this technique involves the formation of four intermediate phases starting with DMF solvate of H_4HDTA, crystallization of polymer, $Zn(H_2HDTA)(DMF)_2(H_2O)$, conversion of this structure to a monoclinic polymorph by continuous grinding and finally formation of MOF-74 with high crystallinity after 70 min of milling.

2.5. Electrochemistry

Electrochemical technique provides a very rapid method for the synthesis of MOFs because of its advantages such as mild reaction conditions, minimal time and controllable parameters during the synthesis.[80,81] Yang *et al.*[82] developed an *in situ* electrochemical synthesis in a tunable ionic liquid (IL) system as electrolyte, under the influence of electric field to prepare MOF-5 (IL) $(Zn_4O(BDC)_3$ (BDC = 1,4-benzene-dicarboxylate) with good crystallinity simple reaction time, high purity, porosity and surface area.[83,84] The MOF-5(IL) synthesized presented a spherical morphology, which is due to the π–π stacking interactions, ionic and coordination bonding. In addition, the groups reported the cyclic voltammetry technique that was used to investigate the reduction and oxidation processes. As a result, The zinc metal is oxidized to Zn^{2+} ions, which go into the solution to react with organic groups existing in it to form MOFs.[85] The reduction peak corresponds to the reduction of Zn^{2+} in metal Zn. The electrochemistry results indicated two successive two-electron redox processes with irreversible reactions. The cyclic voltammetry indicated that shift of the anodic peak potential is in a positive direction and the cathodic peak potential is in a negative direction. In another approach, Wei *et al.*[86] developed a simple and economic electrochemical method to prepare a porous Zr-MOFs, UiO-66-NH_2 with good crystallinity, specific morphology and high surface area at ambient temperature and atmospheric pressure, using zirconium metal, mixture of DMF and 2-aminoterephthalic acid (NH_2-BDC), acetic acid and tetrabutylammonium bromide (TABA) as electrolyte under the influence of electric field to accelerate the reaction. They reported that the sacrificial anode was created from Zr metal, also the cathode has been made by the same metal.

In this technique, the solvent, electric pressure and time of reaction could be taken into consideration for the formation of MOFs by an electrochemical method.[87] Therefore, the results show that the DMF/acetic acid ratio of 52 : 8 led to polyhedron particles, the electric pressure between 4/10 V and time reaction of 1 h were sufficient to obtain a small particle with good crystallinity.

3. Properties and applications

MOFs are known for their polyvalence and adaptability. Several hybrid combinations may be possible to target specific objectives. The elevated porosity and high specific surface area distinguish MOFs from other previous materials like zeolites.[88] The properties of MOFs can be improved by revising the construction by establishing secondary building units called SBU allowing the formation of bonds between organic linkers resulting in another family of MOFs; IsoReticular Metal–Organic Frameworks (IRMOF). The initiation of SBU positively affects the thermodynamic and mechanical stability of MOFs resultant the presence of strong covalent bonds.[89] The pore reactivity of MOFs can be controllably modified through their post-synthetic modifications, a property that is particularly important for catalytic applications. Furthermore, due to their high thermal stability, MOFs exhibited the presence of strong bonds such as M–O, C–H, C–C, and C–O, making them very interested choices for carbon capture processes.[90,91] MOF-2 studied in the literature exemplify the potential of the SBU route ach in fabricating stable porous MOF structures (Fig. 3).[92] To conclude, by reason to obtain MOFs with high porosity, it is very important to choose linkers.[93–95]

MOFs retain high surface area, chemical functionality, largely pervious structure, and adjustable functional groups which give the utilization of MOFs[96] in multitudinous applications as shown in Fig. 4 . In this regard, MOFs have been utilized in gas storage[97,98] and separation,[99,100] photo-catalysis,[101,102] biomedicine[103,104] and chemical sensing.[105,106] MOFs reported to

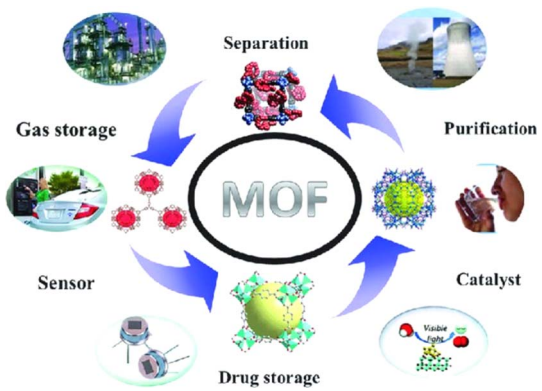

Fig. 4 Widespread potential applications of MOFs. Reproduced with permission from ref. 110 Copyright © 2013, Royal Society of Chemistry.

be more sensatory to humidity owing to the affinity of the metal–ligand bond and thus have not been frequently used for suchlike function. One of the best illustrations has been found to be MOF-5, which degrades regularly when exposed to moisture.[107] Through continuous efforts of searchers, water stable MOFs have been improved and employed in water treatment utilization.[108] Generally, water-stable MOFs can be classified into 3 major categories: (a) hypervalent metal ions incorporated into metal carboxylate frameworks, such as UiO-66, (b) nitrogen donors incorporated into metal azo compound frameworks ligands, such as ZIF, and (c) MOFs constructed with obstructed metal ions are functionalized.

Therefore, many investigator groups have been working on the research of water stable materials. In this way, MOFs are becoming reliable next-generation efficient water treatment materials and can be utilized as adsorbents.[109,110]

4. Adsorption of heavy metals

4.1. Mechanism

The adsorption of heavy metals was developed as an effective method for wastewater remediation. This technology is a simple, eco-friendly and environmentally solution. In addition, the process depends on different chemical and physical properties such as pH, temperature, time of contact between the adsorbent and contaminant, amount, surface area and size of the adsorbent, *etc*[111,112].

In most cases, the adsorption is categorized as physical, chemical, and electrostatic adsorption[113,114] as shown in Fig. 5. Thus, the physical adsorption is characterized by the interactions between the MOFs and the adsorbates on the surface by the van der Waals forces.[115] Whereas, the chemical adsorption or the chemisorption, is caused by the creation of chemical bonds between the adsorbed molecules and the active sites of the surface of the adsorbent by covalent, ionic, and hydrogen bonding.[116] Thus, the chemisorption needs a long time of contact between the adsorbent and the adsorbate because of its strong bonding attachment, whereas the physical adsorption need a short contact time.[117]

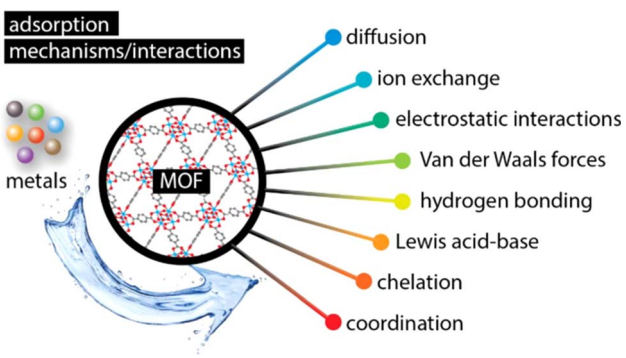

Fig. 5 A schematic illustration of the interactions/mechanisms involved in the adsorption of metals by metal–organic frameworks (MOFs). Reproduced with permission from ref. 114 Copyright © 2013, MDPI.

Metal–Organic Frameworks (MOFs) offer a promising avenue for heavy metal removal from water. These highly tunable materials act like microscopic sieves, their porous structures selectively capturing specific metal ions based on size and charge. Strategically incorporated functional groups within the MOFs further entice these metal ions through electrostatic interactions, culminating in strong chemical bonds that lock them away.[118–122] This approach ensures both efficiency and selectivity in pollutant removal, contributing to cleaner and healthier water resources. By leveraging the unique design flexibility of MOFs, researchers continuously refine these captivating materials, propelling them towards real-world applications in environmental remediation. In fact, Wang *et al.*[123] prepared a magnetic Zr-MOF (Fig. 6).

They examined the adsorption mechanism of lead and chromium in aqueous solution. This innovative as-synthesized demonstrated both excellent thermal stability and strong magnetic properties, enabling convenient separation from treated water after adsorption. It showcased impressive capture abilities, adsorbing up to 273.2 mg g^{-1} of Pb(II)) at pH 4.0 and an even higher 428.6 mg g^{-1} of Cr(VI) at pH 3.0 based on mathematical modeling. Additionally, the adsorption process was incredibly fast, reaching equilibrium within just 60 minutes for Pb(II) and 30 minutes for Cr(VI). Further analysis revealed that the adsorption followed a pseudo-second-order model, indicating specific chemical interactions between the metal ions and the material's surface. These combined features highlight the significant potential of this material for efficiently eliminating heavy metals from contaminated water sources. This material exhibited impressive selectivity, effectively prioritizing capture of target heavy metals even when other ions were present. Furthermore, it displayed remarkable reusability, maintaining significant binding capacity even after five regeneration cycles. By analyzing various techniques like FTIR, XPS, and examining the material's electrokinetic properties, researchers proposed mechanisms for how the material captures lead and chromium as shown in Fig. 7.

They suggest that Pb(II) likely binds through chelation, while Cr(VI) adsorption potentially involves a combination of electrostatic attraction, chelation, and even a redox reaction as illustrated in Fig. 8. This detailed understanding of the adsorption mechanisms paves the way for further optimization and advancement of this material for efficient and sustainable heavy metal removal.

In this sense, Scanning Electron Microscopy (SEM) plays a critical role in deciphering the surface properties of Metal–Organic Frameworks (MOFs), unveiling their potential as powerful adsorbents for pollutant removal. This microscopy technique offers invaluable insights into morphology, revealing the shape and size of individual MOF particles, which can influence their aggregation behavior and ultimately, adsorption capacity.[124] By peering deeper, high-resolution SEM images allow researchers to explore the intricate network of pores within the MOF structure, with their size and distribution directly impacting the efficiency of pollutant capture.[125] But SEM doesn't stop there. It meticulously examines the surface features like roughness, texture, and even defects, all of which

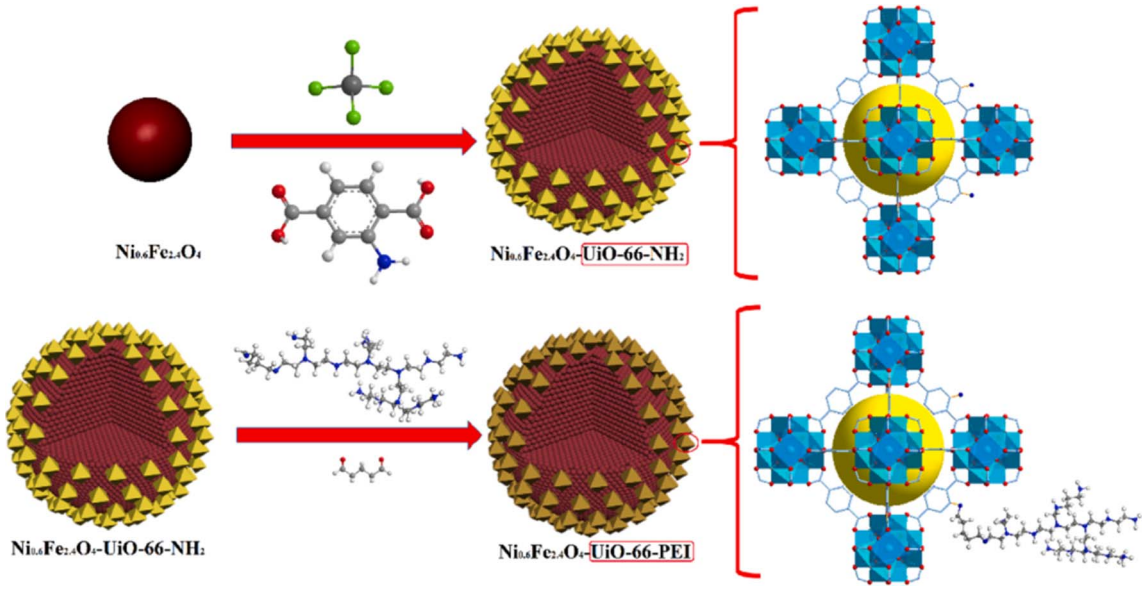

Fig. 6 A schematic showing the procedures to synthesize $Ni_{0.6}Fe_{2.4}O_4$-UiO-66-types. Reproduced with permission from ref. 123 Copyright © 2021, Elsevier.

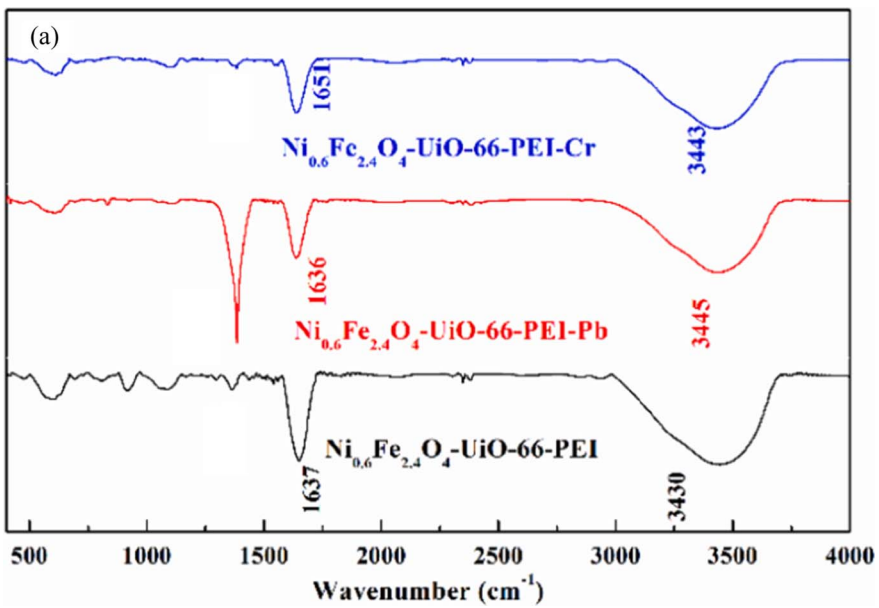

Fig. 7 FTIR spectra of $Ni_{0.6}Fe_{2.4}O_4$-UiO-66-PEI before and after its adsorption of Pb(II) or Cr(VI) (a). Reproduced with permission from ref. 123 Copyright © 2021, Elsevier.

can influence the interaction between the MOF and targeted pollutants.[126] Furthermore, combining SEM with Energy-dispersive X-ray spectroscopy (EDS) generates elemental maps, revealing the presence and distribution of elements within the MOF structure, including impurities or functional groups that can play a crucial role in adsorption mechanisms.[127] In some specialized techniques like Environmental SEM (ESEM), researchers can even directly observe the dynamic interaction between the MOF surface and adsorbed pollutants, offering precious insights into the entire adsorption process.[128] Ultimately, by correlating these observed surface properties with the MOF's adsorption capacity and selectivity towards specific pollutants, researchers gain a deeper understanding, which can guide further design and optimization of these promising materials for environmental remediation.[129,130]

In addition, the researchers reported that the adsorption kinetics measured the rate of the chemical reaction on the adsorbate–adsorbent interface. Thus, the most commonly kinetic models are the pseudo-first order, pseudo-second order, Elovich, *etc*.[131] Besides, the adsorption equilibrium isotherm is

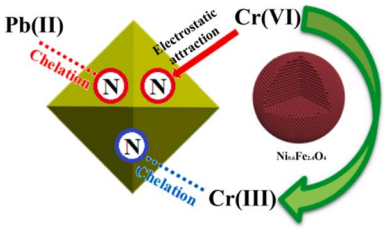

Fig. 8 Adsorption mechanism of $Ni_{0.6}Fe_{2.4}O_4$-UiO-66-PEI for lead and chromium (The N in the circle represents the nitrogen-containing functional group on the surface of $Ni_{0.6}Fe_{2.4}O_4$-UiO-66-PEI). Reproduced with permission from ref. 123 Copyright © 2021, Elsevier.

beneficial to provide more information to describe the adsorption mechanism, because it revealed the interaction between the heavy metals adsorbed by MOFs and the quantity of adsorbate that can be tolerated for adsorption on the surface.[132] Hence, numerous isotherm models were used to explain this adsorption mechanism, such as Langmuir,[133,134] Freundlich,[135] Jossens,[136] Hill,[137] *etc.*

4.2. Heavy metals

Heavy metals present a significant health risk to humans and wildlife. They can accumulate in the tissues of organisms, causing various health problems such as neurological disorders, cancer, and organ damage.[138] Furthermore, these elements can also affect aquatic ecosystems by interfering with the natural food chain and harming sensitive species.[139] Besides, it is challenging to transform them in water into friendly product by biodegradation, referred to organic contaminants.[140] Some of the extremely common heavy metals found in water include lead (Pb), arsenic (As), mercury (Hg), cadmium (Cd), chromium (Cr), and copper (Cu). These heavy metals can come from various sources, such as industrial effluents, agricultural runoff, mining activities, and natural weathering of rocks and soils.[141] Human activities, as improper disposal of hazardous wastes and oil spills impact water sources.[142] Once these heavy metals enter the water cycle, they can remain there for a lengthy time and bring significant problems to both human health and the environment.[143] Table 2 summarizes the permissible values exposure limits for heavy metals by diverse offices and different health problems generated by them.

The reduction of toxic metal ions remains a strong challenge. Therefore, the exploration of suitable techniques for the reduction of heavy metal ions from water sources is recommended.[176] Numerous methods could be utilized to eliminate heavy metal ions, suchlike as adsorption, chemical method, resin ion exchange method and so on.[177] Among them, adsorption is the commonly technique for eliminating metal ions through its low cost, large surface area, ease of handling, and high efficiency with minimal release of by-products.[178–180] Kinetic and thermodynamic effects are very important in the adsorption process. They allowed the study and the comprehension of the complete mechanism. The importance is specially to stimulate the properties of MOFs like adsorption capacity, stability, selectivity and reusability.[181,182] Traditionally, distinct adsorbents like as coal,[183–185] minerals,[186–188] macromolecules,[189] and biomass[190] have been used to eliminate heavy metals, conventional adsorption materials include metal oxides,[191,192] zeolites,[193] carbon materials,[194,195] organic resin,[196] *etc.* Absence of selectivity is the principal inconvenient of the adsorbents already mentioned.[197] Moreover, presence of the random pores decreased the kinetics process due to the reduction transport of the target metal ions.[198] In addition, due to the weak coordination chemistry between metal ions and linkers, treatments such as acidification and impregnation with some unique groups are required to improve the adsorption capacity and selectivity.[199] For instance, zeolites showed a poor selectivity and slow adsorption kinetics,[200] carbon materials had small pore sizes,[201] and organic resin found to be not reusable.[202]

Metal–Organic Frameworks (MOFs) have emerged as intriguing alternatives to established adsorbents like activated carbon, zeolites, and biochar. While each material possesses

Table 2 Heavy metals exposure and major health impacts[a]

	Standards (mg L^{-1})			
Heavy metals	WHO[144,145]	USEPA[146]	BIS[147]	Health problems
Arsenic	0.010	0.010	0.05	Arsenicosis, psychological effects,[148–150] reduced mental efficiency,[151] hypertension, cardiovascular sickness, carotid, and diabetes,[152–155] lung cancer,[156] carcinogenesis[157]
Cadmium	0.003	0.005	No relaxation	Neurodegenerative,[158] ESRD,[159] cancers,[160,161] [demineralization of bones[162] diabetes[163]
Mercury	0.006	0.002	No relaxation	Intestinal disorders, urinary problems, paralysis, tyrosinemia, intoxication[164]
Lead	0.01	0.00	No relaxation	Neurotoxic problems[165] reduced memory[166] anemia [167] cyclic vomiting syndrome[168] toxicity[169] cancers like lung cancer[170]
Chromium	0.05	0.1	No relaxation	Bronchitis, mutagenic results[171,172]
Copper	2.0	1.3	1.5	Alzheimer, cirrhosis[173,174]
Zinc	5.0	—	15	Gastroenteritis fever, pulmonary pain[175]

[a] WHO (world health organization), USEPA (United States Environmental Protection Agency), and BIS (Bureau of Indian Standard).

unique advantages and drawbacks, understanding their comparative strengths across various aspects is crucial for informed selection:

Economics: MOFs currently suffer from higher synthesis costs compared to readily available adsorbents like activated carbon.[203] However, recent efforts towards cost-effective methods and scalable production hold promise for bridging this gap.[204]

Environmental Impact: MOFs frequently boast superior adsorption capacities and selectivity, translating to reduced waste generation and water usage compared to other adsorbents.[205] Additionally, their tunable design allows for the minimization of harmful chemicals during synthesis, contributing to a greener approach.

Practicality: regeneration, a key factor for sustainability, presents a challenge for some MOFs due to their intricate structures and potential sensitivity to harsh desorbing agents.[206] While activated carbon and zeolites offer simpler regeneration processes, their lower capacities may necessitate frequent replacements.[207]

Other Considerations: MOFs offer unmatched tunability, enabling researchers to tailor their properties for specific metals and environmental conditions.[208] Their unique structures can also be functionalized for additional functionalities like separation and catalysis.[209] However, large-scale implementation requires further research on their mechanical strength and long-term stability under real-world conditions.

For the time being, MOFs have been devoted to reduce heavy metal ions from polluted water since of their superb adsorption capacity to reduce toxic metals from polluted water.[210,211] In this section, we discussed the most powerful MOFs for the reduction of toxic metals, cadmium, arsenic, chromium, mercury, and lead. There are several types of MOFs being studied for heavy metals removal such as ZIF-8, MIL-101, UIO-66, IRMOF and MOF-74. These MOFs have unique structures and characteristics that make them promising candidates for effective and efficient reduction of heavy metals.[212]

Photocatalysts based on MOFs have found immense importance in the remediation to treat polluted water and other applications. In this context, Dhivya *et al.*[213] designed the MOF NTU-9/NH_2-MIL-125 composite (HMF) using the return method. Compared with NTU-9, HMF's thermal stability is increased to 520 °C. The researchers studied the ability to reduce Cr^{2+} from contaminated water. They found that the maximum capacity reached 50% of the restore. In sync, the acid state prefers Cr(VI) reduction and HMF to reduce 100% within 90 minutes after visible light radiation. Further, Ghanbari *et al.*[214] synthesized a composite MOFs from produced metal–organic framework-101 *via* the *in situ* growth method. The authors found that the rejection percentage of five different genres of heavy metal ions such as Cd(II) denoted more than 95%. Nowadays, multifunction MOFs are currently attracting researchers because they can be utilized to detect and eliminate heavy metals in the aquatic solution. In this way, Rudd *et al.*[215] by incorporating a strong molecular fluorescence and functional common lines in the structure based on Zn, fabricated a series of light emitting metal organic frameworks (LMOF). The microporous materials were LMOF-261, -262 and -263. They found that the fluorescent MOF-263 had stately water stability, high pore rate and strong luminescence, which had led to good applicants as fluorescent chemical sensors and as an adsorbent of heavy metals at the same time. Also, they showed that this material exhibited a higher adsorption capacity corresponding to 380 mg_{Hg2+} g^{-1}. Demonstrating the importance of recyclability in environmental remediation, researchers explored LMOF-263, a material that effectively captures and releases harmful mercury (Hg^{2+}). Unlike traditional harsh acidic methods, they successfully employed a two-step CS2 extraction process followed by structural analysis, revealing that the material retained over 92% of its original structure even after two full adsorption–desorption cycles. This promising finding suggests the potential of LMOF-63 for sustainable Hg^{2+} removal, paving the way for further development of environmentally friendly remediation methods. Previously, Zhou *et al.*[216] synthesized a material PVDF@MOF-303 membrane. They showed that the as-prepared for toxic heavy metal ions adsorption. In addition, after cycles, a separation efficiency of 93.0% was obtained. Similarly, Zhao *et al.*[217] developed a new composite nanocellulose aerogel@MOF-801 for efficient Cr(VI) adsorption. They demonstrated that the adsorption efficiency of this composite for Cr(VI) was 93.86%. Besides, the maximum adsorption of chromium was 350.64 mg g^{-1}. Furthermore, the composite showed good reusability, with no significant loss of adsorption performance over 6 cycles. In another work, Zhang *et al.*[218] prepared a recyclable adsorbent citric acid modification β-cyclodextrin metal–organic framework to remove heavy metals. Consequently, the adsorption capacities for the copper ions were as high as 287.4 mg g^{-1}. As result, the CA-β-CD-MOF prepared has good adsorption performance and recyclability and has great potential in removing heavy metals from aqueous solution. As follows, Zhang *et al.*[219] synthesized a novel nanocomposite hydrogel@MOF-5 to remove lead ions from water. They showed that the as-prepared exhibited maximum adsorption capacities for Pb(II) of 189 mg g^{-1} at pH 6. In addition, the recyclability of MOF-5/PNaSS/SA, as its adsorption capacity remained at a high level after ten cycles.

4.2.1. Cadmium removal. Cadmium is a toxic heavy metal that can have dangerous risks to both human health and the environment.[220] Here are some of the risks associated with cadmium exposure: (i) health risks: cadmium exposure can guide to a range of diseases, including kidney damage, lung damage, and cancer. Extended exposure to low levels of cadmium can also cause bone demineralization, leading to osteoporosis.[221] (ii) Environmental risks: cadmium can contaminate soil, water, and air, and can have harmful effects on plants and animals. It can accumulate in the food chain, leading to high levels in some fish and shellfish.[222]

Some common sources of cadmium include industrial activities such as mining and refining,[223] food,[224] drinking water[225] and fertilizers.[226] Overall, MOFs have been shown to be effective for the elimination of both cadmium from polluted water sources, and continued research in this area could lead to the progress of more efficient and cost-effective treatment techniques for these harmful contaminants. Zhang *et al.*[227] prepared

a functionalized zinc-based MOF named HS-mSi@MOF-5 to adsorb Cd(II) ions through the thiol functionalization. They found that the adsorption capacity of the composite was 312.5 mg g^{-1}. In contrast to MOF-5, superior adsorption outcomes were observed. Furthermore, MOF-5 exhibited instability in acidic solutions, as confirmed by a hydrostability test. Consequently, the thiol groups enable a coordination interaction with cadmium ions. Roushani *et al.*[228] prepared the TMU-16-NH_2 another zinc-based MOFs by solvothermal method. In this work, the team studied the adsorption of trace amounts of cadmium ions. They realized that the maximum adsorption capacity of Cd(II) ions determined to be 126.6 mg g^{-1}. Following the thermodynamic parameters, the reaction is endothermic and spontaneous. In other research, Jamshidifard *et al.*[229] prepared a PAN/chitosan/UiO-66-NH_2 composite nanofibers *via* electrospinning as shown in Fig. 9. They found that the maximum monolayer adsorption capacity of the nanofibrous adsorbent for Cd(II) ions sorption was 415.6 mg g^{-1}, under optimum conditions (MOF content: 10 wt%, pH 6 Cd(II), equilibrium time 1 h, and temperature 25 °C).

Binaeian *et al.*[230] synthesized a ZIF-8 modified by dimethylethylenediamine (ZIF-8-mmen). The satisfactory results were obtained when pH, dosage, and time were 2, 0.1 g, and 89 min, correctly, with eliminate efficiency of 85.38%. Whitin this study, Liu *et al.*[231] prepared an ecofriendly γ-cyclodextrin MOF-based nanoporous carbon (γ-CD MOF-NPC) by a mild and simple crystallization method at room temperature. They displayed that the maximum adsorption capacity was 140.85 $mg_{Cd(II)}$ g^{-1}. Yusuff *et al.*[232] reported a copper-based metal–organic frameworks method to reduce cadmium ions polluted water. They determined that the maximum adsorption capacity was 219.05 mg g^{-1}. Mahmoud *et al.*[233] synthesized meso-porous amino-decorated magnetic by modification of based iron MOFs (MIL-88) using a microwave-assisted technique. They found that the maximum adsorption capacity of cadmium(II) ions was 693.0 mg g^{-1}. The regeneration of *n*Fe_3O_4@MIL-88A(Fe)/APTMS proved to be straightforward, with adsorptive removal values decreasing by merely 3% after five consecutive recycling processes. High recovery rates were achieved in tap water, sea water, and wastewater for Cd(II) removal, measured at 98.49%, 96.22%, and 94.73%, respectively. The removal of Cd cations was achieved through coordinate bond formation, particularly effective at pH levels exceeding 4 due to the functionalization of the composite material. Abo El-Yazeed *et al.*[234] successfully produced a bimetallic Ag–Fe metal organic framework. The authors showed an extraordinary Cadmium(II) adsorption capacity of 265 mg g^{-1}. As a result, the optimal outcome is achieved with a 0.6 : 1 ratio of Ag–Fe MOF, attributed to a pronounced synergistic effect between the two metals. Notably, the catalysts based on metal–organic frameworks retained both their adsorption capacity and catalytic activity even after undergoing four cycles of reuse. Kim *et al.*[235] fabricated a copper-based MOF as highly attractive candidate water stability (Fig. 10). They observed an excellent adsorption of Cd(II) ions higher than 100 mg g^{-1} and regeneration efficiency of 90%. Therefore, the advantage of this study is to be able to separate between the metals to be adsorbed by increasing the selectivity with appropriate redox reaction.

Recently, Singh *et al.*[236] produced a calcium fumarate MOF. The as-synthesized MOF was employed for reduction of Cd(II). In this study. The authors found that the adsorption capacity of CaFu MOFs was 781.2 $mg_{Cd(II)}$ g^{-1}. Hence, CaFu MOFs exhibited stability in both neutral and alkaline environments but dissolve in acidic conditions, leading to the breakdown of the organic framework into CO_2. Even after undergoing five cycles, the desorption percentage of Cd(II) remains high at 80.9%. In another study, Ahmadijokani *et al.*[237] prepared an ethylenediamine-functionalized zirconium-based metal–organic framework called UiO-66-EDA *via* Michael reaction. Kinetics parameters showed that the functional MOF had a maximum adsorption capacity of 217.39 $mg_{Cd(II)}$ g^{-1}. Further, the adsorption mechanism of Cd onto UiO-66-EDA was physical and chemical sorption. Abdelmoaty *et al.*[238] investigated on UiO-66 modified consequently with melamine. The authors

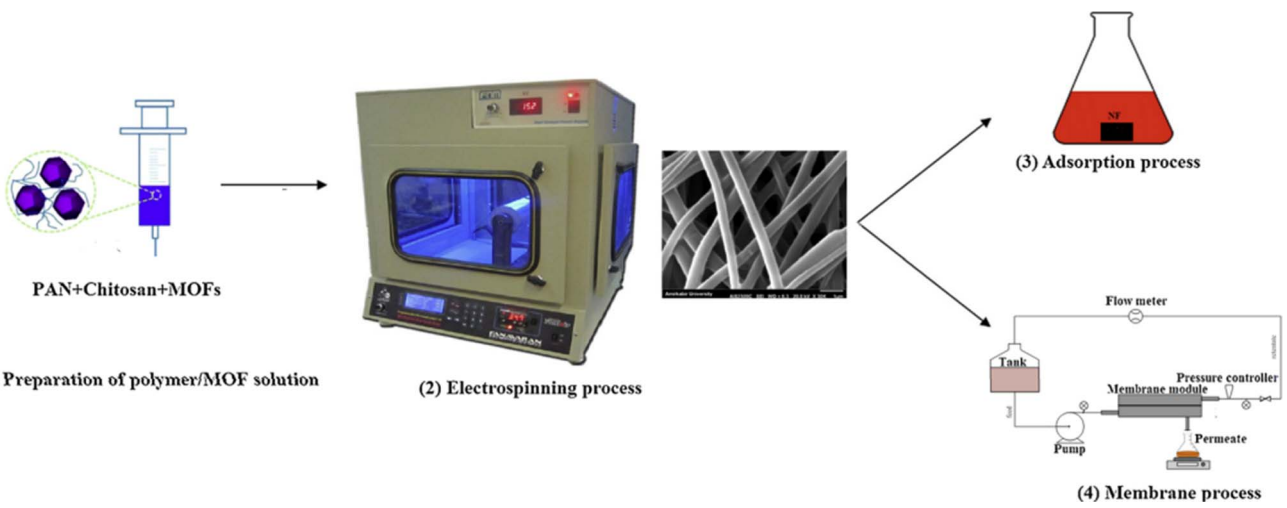

Fig. 9 Illustration of the fabrication of nanofibers/MOFs and its application for the removal of metal ions. Reproduced with permission from ref. 229 Copyright © 2019, Elsevier.

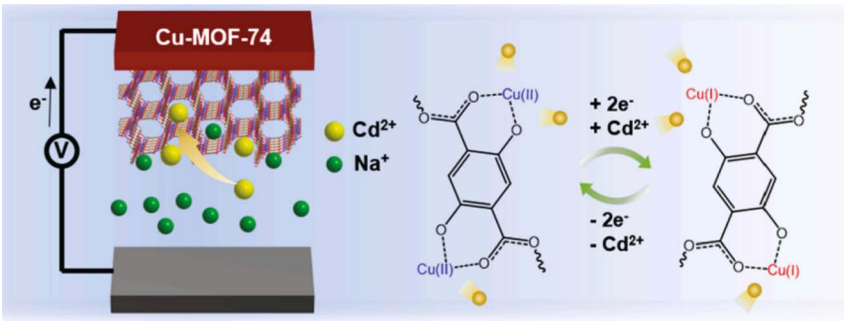

Fig. 10 Schematic representation of the electrochemically assisted capture of cadmium ions. Reproduced with permission from ref. 235 Copyright © 2021, Elsevier.

observed a notable adsorption capacity of 146.6 mg g^{-1} for Cd(II) ions. They found that the UIO-66 modified achieved for three cycles by MUiO-66. Following the last research, Gul *et al.*[239] prepared zirconium-based MOFs with SO_3H functionalization (UIO-66-SO_3H) stable in water. They found that the maximum adsorption capacity of Cd(II) was 194 mg g^{-1}, at an initial concentration of 1000 mg L^{-1}. Abdel-Magied *et al.*[240] coordinated two magnetic composites MOFs by coprecipitation method with a simple modification. In addition, Fe_3O_4@UiO-66–NH_2 and Fe_3O_4@ZIF-8 exhibited a maximum adsorption of cadmium ions of 714.3 mg g^{-1}, and 370 mg g^{-1} for Cd(II), properly at pH 7. Besides, the as-synthesized magnetic adsorbents kept a similar response in four continuous cycles. In this context, UIO-66 had always demonstrated excellent heavy metals adsorption capacity.

To summarize we have presented in Table 3 some potential MOFs for cadmium removal.

4.2.2. Arsenic removal. Arsenic is a toxic element that can cause a range of diseases and environmental issues.[256] In humans, exposure to elevated levels can lead to skin problems, and attack other organs, like cardiovascular disease, diabetes, and other chronic diseases. It may also affect the development of the nervous system, leading to cognitive impairment, behavioral changes, and other neurological disorders.[257–259] In the environment, arsenic can contaminate water,[260] soil,[261] and air,[262] leading to serious ecological problems. It can harm aquatic life, damage ecosystems,[263] and reduce biodiversity.[264] Arsenic pollution can also affect agricultural productivity, as it can accumulate in crops and food chains, leading to food safety issues.[265] To address the health problems and environmental issues related to arsenic, various measures are needed, such as reducing arsenic emissions from industrial sources, improving waste disposal practices, promoting safe drinking water, and encouraging sustainable agriculture. MOFs have emerged as promising materials for the adsorption of arsenic due to their high surface area, tunable pore sizes, and excellent chemical stability. Some recent research papers quoted in the following paragraphs, showed the potential of MOFs for arsenic removal.

Li *et al.*[266] prepared by microwave technique zirconium-based MOFs nanoparticles to reduce arsenic from polluted water. They showed that the maximum adsorption capacity of material for arsenic was 24.83 mg g^{-1}. In addition, the as-prepared is an efficient adsorbent after five cycles of utilization. Huo *et al.*[267] fabricated a water stable Fe_3O_4@ZIF-8 composites by a facile modification (Fig. 11). The authors showed that as-obtained composite reached a maximum adsorption capacity of 100 $mg_{As(III)}$ g^{-1}. Following the thermodynamics parameters, the reaction was spontaneous and endothermic.

Sun *et al.*[268] reported a novel Fe–Co microporous material (MOF-74) for the removal arsenic in water. They found that the composite had an excellent adsorption concerning As(III) and

Table 3 Potential MOFs for cadmium adsorption

Heavy metal	MOFs	pH	Adsorption capacity (mg g^{-1})	Contact time (min)	Ref.	Other adsorbents: Adsorption capacity (mg g^{-1})
Cd(II)	MOF-88/PAN	—	225.05	10	241	Graphene oxide (0.64),[242] peels of banana
	UiO-66-EDA	7	217.39	360	249	(5.71),[243] *Eichhornia crassipes*
	Fe_3O_4@MOF-235(Fe)–OSO_3H	3	163.9	5	250	biomass (104),[244] sulfur-functionalized rice-husk
	ED-MIL-101(Cd)	8	63.15	180	251	(137.16),[245] magnetic carbon aerogel (143.88),[246] I–Al_2O_3-
	NH2–Zr-MOF	6	177.35	—	252	nanoparticles (66),[247]
	TMU-5	10	634	1440	253	calcium alginate-nZVI-biochar composite (47.27)[248]
	nFe_3O_4@MIL-88A(Fe)/APTMS	6	693	60	254	
	TMU-16-NH_2	126.6	6	30	255	

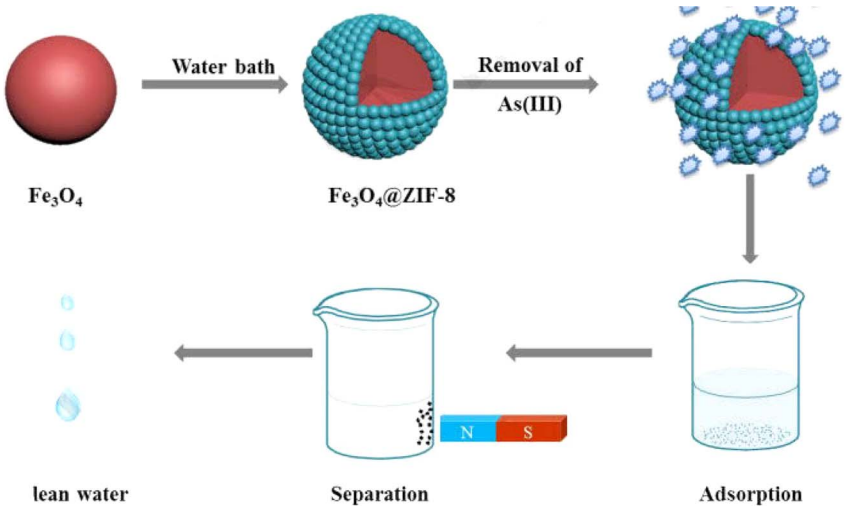

Fig. 11 Preparation of magnetic MOFs composite for separation after efficient elimination of As(III) from water. Reproduced with permission from ref. 267 Copyright © 2018, Elsevier.

As(v) of 266.52 and 292.29 mg g^{-1}, property. Li *et al.*[269] prepared iron-based MOFs called MIL-101-Fe *via* a facile solvothermal method. They showed that the material presented a maximum adsorption capacity for As(v) of 232.98 mg g^{-1}. Yu *et al.*[270] made a Zn-MOF-74 by solvothermal synthesis to eliminate both As(v) and As(III). They discovered that the crystal had a significant adsorption capacity of 325 mg g^{-1} and 211 mg g^{-1} of As(v) and As(III), appropriately. Similarly, Zhao *et al.*[271] designed an ultrathin two-dimensional zeolitic imidazolate framework 67 (ZIF-67-Nanosheets) to study the process of elimination of As(III). They showed that the as-synthesized ZIF-67-NS had a higher adsorption capacity of 516 mg g^{-1}. In addition, the material showed the same adsorption capacity after 3 cycles. In other research, Liu *et al.*[272] reported a titanium uniform-sized and microporous MOF to improve arsenic elimination. They demonstrated that the top adsorption capacity of As(III) and As(v) were 40.26 and 46.34 mg g^{-1}, properly. Yang *et al.*[273] designed a spindle MOF composite able to remove As(III) from contaminated water by a simple *in situ* synthesis approach with the modified of structure of Fe–Co-MOF-74. They showed that the composite had high adsorption rates in the pH range of 2–10 and the biggest adsorption capacity value of As(III) was 300.5 mg g^{-1}. Song *et al.*[274] prepared a new MOF by assemblage of hexanuclear Zr-oxo clusters. They found that the maximum adsorption capacity for As(v) to be 153.48 mg g^{-1} in an acidic media. More importantly, the as-synthesized treated polluted water with only trace arsenic pollution. Pervez *et al.*[275] designed two cerium-based metal–organic frameworks towards arsenic species from water. They found that the maximum adsorption capacities of As(v) by cerium-MOF-66 and cerium-MOF-808 was 355.67 and 217.80 mg g^{-1}, respectively. For As(III) was 5.52 and 402.10 mg g^{-1} for Ce-MOF-66 and Ce-MOF-808, properly. In the following work, Kalimuthu *et al.*[276] investigated the efficacy of removing arsenate by MOFs derived from recycled bottles. They found that at the 70.02, 85.72 and 114.28 mg g^{-1}, the maximum adsorption capacity of arsenate on Fe-MOF, Zr-MOF and La-MOF, properly was at PH 7. Besides, the as-prepared MOFs were effectively reclaimed after 5 cycles. Whereas, Li *et al.*[277] have prepared a FeS_x@MOF-808 composite to reduce As(III) from polluted water. They demonstrated that the material exposed the maximum As(III) adsorption capacity to the surrounding of 203 mg g^{-1} at 25 °C and neutral pH. Li *et al.*[278] have designed a novel nanocomposite-based MIL-53 to enhance the water stability of the composite. They demonstrated that the maximum adsorption capacity was 27.24 mg g^{-1} in a low As(v) concentration of 10 mg g^{-1} (Fig. 12).

To recap we have presented in Table 4 some potential MOFs for arsenic elimination.

4.2.3. Mercury removal. Mercury is a toxic heavy metal and in water is a pressing environmental issue characterized by a potent neurotoxin in aquatic ecosystems. This contamination often stems from industrial discharges, mining activities, and natural processes like volcanic eruptions. Once introduced into water bodies, mercury undergoes complex transformations, cycling between the atmosphere, water, and sediments. The impacts of mercury toxicity include neurological and developmental disorders, especially in vulnerable populations like pregnant women and children. Stringent monitoring, regulatory measures, and global efforts to reduce mercury emissions are essential to mitigate the adverse effects of mercury toxicity in water and safeguard both ecosystems and human health.[297,298] In this context, MOFs have been shown to be potential materials for the elimination of mercury from contaminated water sources.

In this instance, Abd El Salam's *et al.*[299] reported the elimination of mercury *via* Mn-MOF which exhibited adsorption efficiency of 65.19%. In other work Xiong *et al.*[300] explored unmodified MOF-74-Zn material to remove mercury ions from aqueous solution. They demonstrated that pH value, time, initial concentration of Hg^{2+} and temperature had an effect on Hg(II) uptake by the adsorbent. Therefore, the removal efficiency increased with increasing pH up to 6 and it remained constant.

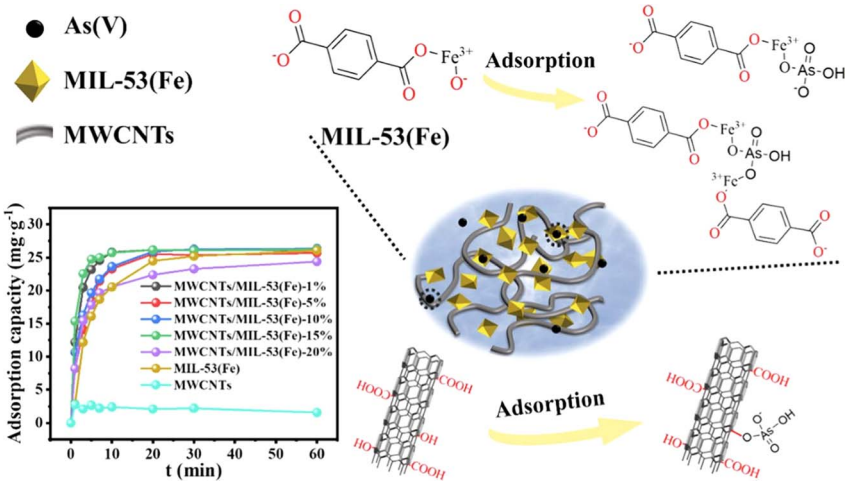

Fig. 12 Schematic of adsorption process and performance of the nanocomposite MWCNTs@MIL-53(Fe) to remove As(v) from polluted water. Reproduced with permission from ref. 278 Copyright © 2023, Elsevier.

Table 4 Potential MOFs for arsenic removal

Heavy metal	MOFs	pH	Adsorption capacity (mg g^{-1})	Contact time (min)	Ref.	Other adsorbents: Adsorption capacity (mg g^{-1})
As(v)	UiO-66	9.2	68	20	279	Fe–Mn-AC (19.35),[280] MPSAC-La (227.6),[281] Ca-alginate beads (42.4),[282] ABA300 (62.9),[283] Fe–Mn loaded zeolite (318)[284]
	UiO-66	2	303	2880	285	
	ZIF-8	—	76.5	720	286	
	ED-ZIF-8	—	83	360	287	
As(v)/As(iii)	Fe/Mg-MIL-88B	7	303	30	288	
	Fe–Co-MOF-74	—	266	360	289	
As(iii)	β-MnO @ZIF-8	7	140.27	—	290	BPC/nZV (177.8),[291] phosphorous-doped GO (157.4)[292] magnetic Fe–Cu-600 (840),[293] Ni-laterite mining waste-derived magnetite (435)[294]
	Fe_3O @MIL-101(Cr)	7	121.5	1440	295	
	Fe–Co-MOF-74	—	266.52	720	296	

The adsorption equilibrium was reached after 1.5 hours. The adsorption efficiency is much better when the temperature is higher. Also, they mentioned that the physisorption and chemisorption both have contributions to the adsorption process of Hg^{2+}. They reported that introducing hydroxyl groups in the pore can coordinate with Hg(ii) ions, which will be considered as strong sites for Hg(ii) chemisorption. The removal efficiency of Hg(ii) by MOF-74-Zn was 54.48%, 69.71%, 72.26% when the initial concentration of Hg(ii) is 20 ppb, 40 ppb, 50 ppb. Also, Zhang *et al.*[301] prepared novel copper-based metal–organic frameworks (Cu-MOFs) which shows a high removal performance of mercury due to porosity, large surface area, good stability, good crystallinity and abundant active sites. They observed an excellent adsorption with an efficiency higher than 90%. Liu *et al.*[302] reported new alkenyl-derived MOFs Cr-MIL-101 s (MIL = material of Institute Lavoisier) by catalytic carbon bond-forming reactions by means of postsynthetic modification (PSM) protocol. They are characterized by particle size, good porosity, large surface area, excellent thermal, chemical stability and high density of adsorption sites, which lead to excellent efficiency of 99.3% when the initial concentration of Hg^{2+} was 10 ppm in 6 h (Fig. 13). Similarly, Yang and coworkers[303] synthesized Zr-MSA MOFs with high activity of alkyl thiol in an aqueous phase which is characterized by particle size, good porosity, excellent chemical stability and strong affinity between alkyl thiol and Hg^{2+} ions. Therefore, they exhibited excellent adsorption performance of 99.99% Hg^{2+} ions in 5 min at range of pH (0–7). Table 5 presented promising MOFs utilized for mercury adsorption.

4.2.4. Lead removal. Lead toxicity in water is a critical environmental concern, stemming from the presence of elevated lead levels that pose serious health risks. Various sources contribute to lead contamination in water, including aging infrastructure with lead pipes, industrial discharges, and historical use of lead-based paints. The toxic effects of lead are particularly alarming, as exposure can lead to adverse health outcomes, especially in children and pregnant women. Ingesting or inhaling lead-contaminated water can result in developmental issues, cognitive impairments, and neurological damage. Efforts to address lead toxicity involve monitoring water quality, implementing infrastructure improvements, and raising public awareness about the risks associated with lead exposure.[317–319] Recently, MOFs have been shown to be potential adsorbents of lead from polluted water.

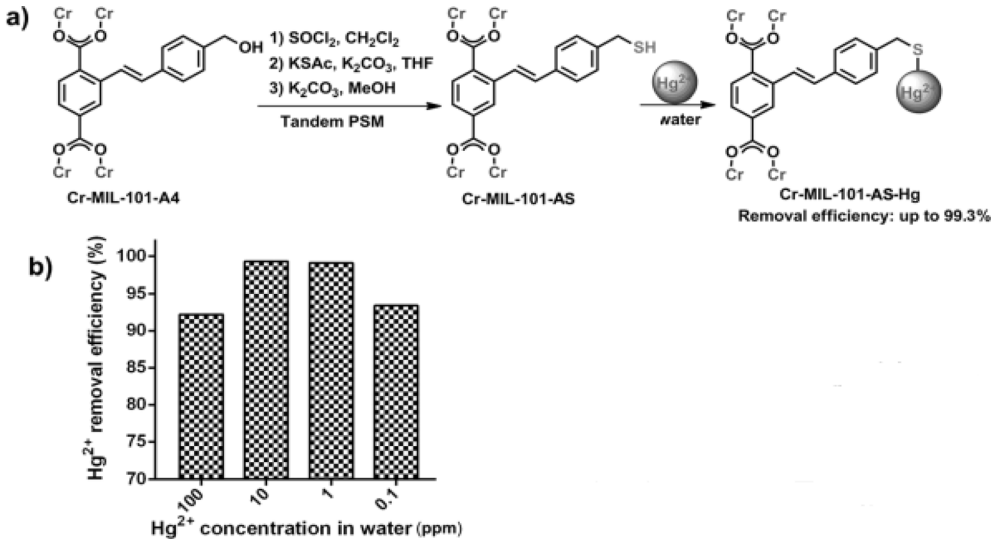

Fig. 13 (a) Post-synthetic modification (PSM) of Cr-MIL-101-A4 to Cr-MIL-101-AS and its application in mercury removal. (b) Mercury adsorption efficiency of Cr-MIL-101-AS in water. Reprinted with permission from ref. 302 Copyright 2014, Wiley.

Table 5 Potential MOFs for mercury removal

Heavy metal	MOFs	pH	Adsorption capacity (mg g^{-1})	Contact time (min)	Ref.	Other adsorbents: Adsorption capacity (mg g^{-1})
Hg(II)	UiO-66-$(SH)_2$	—	236.4	1440	304	Thioglycerol LDH@Fe_3O_4 (480.7),[305] $CoFe_2O_4$@SiO_2-EDTA (103.3),[306] cysteine-carbon/Fe_3O_4 (94.33),[307] curcumin-based magnetic nanocomposite (144.9)[308] Fe_3O_4/hydroxyapatite (492.2),[309] $CoFe_2O_4$/SiO_2/polypyrrole (680.2)[310]
	Zr-MSA	Wide working range	734	5	311	
	Zr-L4		322	1200	312	
	SH-MiL-68 (po))	4	450.36	2	313	
	JUC-62	—	836.7	15	314	
	UiO-66-NHC(S)NHMe	—	769	240	315	
	MOF-808-EDTA	—	592	5	316	

Thus, Yin and co-workers[320] synthesized amino-functionalized metal–organic frameworks (MOFs) combined with ceramic membrane ultrafiltration (CUF), as an effective removal of Pb(II) because of the best reaction between ($-NH_2$) and Pb(II). They highlighted that the adsorption efficiency is much better at pH around 6, at low temperature in case of 30 °C because there are more of available sites. In addition, Shooto *et al.*[321] prepared Cobalt-metal–organic frameworks (Co-MOFs) with irregular size of particles and high crystalline phase. They investigated that large surface area led to maximum adsorption. Also, the presence of (C, O, Co and OH) elements will create charges on the surface, which plays an important role in the adsorption of Pb^{2+}. They observed an excellent sorption of 85% after 20 min at low temperature and lower concentration of Pb^{2+}, due to the availability of more Co-MOF pore.

In another study, Shi *et al.*[322] synthesized new metal organic frameworks (MOFs) composite, CuMOFs/Fe_3O_4 to be used as adsorbent for removal of lead (Pb(II)). The as-prepared materials shows a removal efficiency for Pb(II) of 96% for concentration less than 10 mg L^{-1}. Moreover, Wang *et al.*[323] developed (NH_2)- functionalized Zr-MOFs, characterized by the amino groups ($-NH_2$) which plays the role of Lewis base that will coordinate with Pb(II) (role of Lewis acids). The results of the study showed that the obtained MOFs have high porosity and high surface area. The adsorption capacity of Pb(II) is much higher at lower concentrations (10–20 mg L^{-1}), lower temperature and at range of pH (2–6). Therefore, the removal efficiency of Pb(II) was 99.95% after 120 min at temperature of 30 °C and pH of 6 with an initial concentration of 10 mg L^{-1}. Zhang *et al.*[324] prepared a MOF-PDA-P as an efficient and selective adsorbent for elimination of trace lead from water compared to MIL-100 (Fe). The as-synthesized composite material reached an adsorption rate of 99.35%. Other researchers showed that the synthesis of MOFs based on heavy metals can be effective in eliminating others. In this context, Ghaedi *et al.*[325] synthesized MOF-2 (Cd) as adsorbent for high efficiency removal of lead from aqueous solution. They showed that 1 g of MOF-2 based on cadmium removed 99.9% of lead

for concentration of 200 mg L^{-1} by factorial experimental design under ultrasonic condition. In addition, they demonstrated that the materiel can be used at least three times for the elimination of Pb. Goyal *et al.*[326] demonstrated that the prepared polyacrylic acid capped Fe_3O_4– Cu-MOF (i-MOF) hybrid eliminated 93% of Pb(II) from contaminated water. Furthermore, the adsorption capacity reached 610 mg g^{-1}. Besides 91% of i-MOF could be easily separated from the contaminated water by magnetic separation. Zhu and co-workers[327] developed a nanotube-like Tb-based metal–organic frameworks as a good adsorbent of lead from water. In addition, the as-prepared material exhibited a maximum removal capacity of 547 mg g^{-1} and could maintain a high adsorption performance even after five cycles. N. Abdollahi *et al.*[328] designed Fe_3O_4@TMU-32 metal–organic framework (MOF)-based nanocomposite as an excellent adsorbent to eliminate Pb(II) from polluted water. The prepared material showed a high removal capacity of 45% towards Pb(II). Besides, they demonstrated that the nanocomposite adsorbed 1600 mg g^{-1} of lead in contaminated water. Lately, Ijaz *et al.*[329] synthetized Fe-THC MOF as a selective adsorbent to remove lead from wastewater. They showed that the maximum sorption capability was 674 mg g^{-1} at 305 K and pH 4.5. In addition, the functional Fe-THC MOF by MXene has excellent reusability demonstrated by a greater elimination rate even after five cycles. Table 6 summarized some MOFs able to remove lead.

4.2.5. Chromium removal. Chromium in water is a significant environmental challenge, arising from the presence of elevated levels of chromium, a heavy metal, in aquatic systems. The sources of chromium contamination include industrial discharges, chemical runoff, and disposal of industrial waste. Hexavalent chromium is a concerning form due to its high toxicity and carcinogenic properties. Once introduced into water bodies, chromium can accumulate in sediments and aquatic organisms, entering the food chain and posing a risk to human health. Exposure to elevated chromium levels has been associated with adverse health effects, including respiratory issues and an increased risk of cancer. Monitoring and regulating chromium levels in water sources are crucial to mitigating these risks.[346–348] In this context, Metal–organic Frameworks attracted researchers as an effective adsorbents of chromium removal and reduction from polluted water.

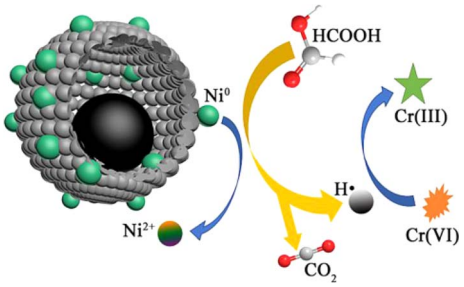

Fig. 14 Catalytic reduction of Cr(VI) by Ni@carbon450 in the presence of HCOOH. Reprinted with permission from ref. 351. Copyright 2020, Elsevier.

In this regard, Mahmoud *et al.*[349] reported the recent advances in application of functionalized MOFs various MOFs composites were assembled and fabricated with some semiconductor photocatalysts as ZnS/CdS/ZnxCd1-xS Ag-based nanoparticles (NPs), ZnO, g-C_3N_4, Bi-based NPs composites as removal materials of Cr(VI). The results gave an efficiency of adsorption in the range of 95.46–99.69%. In another study, Hasan *et al.*[350] synthesized Cu-carbon composite *via* calcination of HKUST-1 at 550 and 650 °C under N_2 atmosphere. The as-prepared material exhibited excellent photocatalytic activity toward Cr(VI) reduction. They investigated rise in temperature destroying the morphology and increasing the surface area. While, Cu@C-550 shows a considerable catalytic reduction of Cr(VI) near to 100% after 15 min in the presence of HCOOH. Also, Lv *et al.*[351] prepared a 3D yolk shell-like structure Ni@carbon composites. The results of the study show that the Ni@carbon450 exhibited excellent performance on the treatment of Cr(VI) due to its large surface area, its mesoporous size and its high concentration of HCOOH (Fig. 14). Thus, the Cr(VI) was completely reduced nearly 100% by Ni@carbon450 in the presence of HCOOH after 30 min at pH 6.

Table 6 Potential MOFs for lead adsorption

Heavy metal	MOFs	pH	Adsorption capacity (mg g^{-1})	Contact time (min)	Ref.	Other adsorbents: Adsorption capacity (mg g^{-1})
Pb(II)	MOF decorated with negatively charged O– groups	6	616.64	—	330	Graphene oxide (5.63),[331] peels of banana (2.18),[332] lanthanum oxide-modified bentonite (147.05),[333] nano zero-valent iron particles-RSAC (140.8),[334] HCO-$(Fe_3O_4)_x$ composite (35.93),[335] sulfur-modified nanoscale zero-valent iron (246.40),[336] MoS2/PDA/MPS (371.7),[337] AA-SW-AMPS (253.49)[338]
	Tb-MOF	3–7	547	50	339	
	Urea-based MOF	5	909	15	340	
	MOF-2	5–6	769.23	60	341	
	IOMN@NH_2-MIL53(Al)	—	492.4	360	342	
	ZIF-8-0	5	1321.21	120	343	
	UiO-66-NH_2	4.5	1795.3	40–45	344	
	UiO-66-NH_2	—	232	240	345	

Besides, Fu and co-workers[352] developed MIL-68 and its derivative hollow porous In_2S_3 with assembled ultrathin nanosheets obtained *via* sulfidation treatment using MIL-68 as a self-sacrifice template. The hollow porous In_2S_3 has great potential for being used for photocatalytic Cr(VI) reduction. The results show that the synthesized materials show a high Cr(VI) removal efficiency near to 100% at pH 6 with low initial concentration of 10 mg L^{-1}. Qing *et al.*[353] designed functionalized material MIL-125(Ti)-amidoxime as efficient adsorbent of Cr(VI) from wastewater. The results show that the as-prepared MOF achieves adsorption capacity of 271 mg g^{-1}. Also, the toxic Cr(VI) can be reduced to Cr(II) species which is beneficial to the process. Yuan *et al.*[354] prepared modified bimetallic Cu@MIL-53(Fe) and used for Cr(VI) elimination. As results, the Cr(VI) removal capacities were 20.65 mg g^{-1} at 180 min and 13.35 mg g^{-1} in 15 min, and 45.55% of total chromium and 99.05% of Cr(VI) were removed at a dose of 0.5 g L^{-1}, pH = 3, 25 °C. Newly, Tan *et al.*[355] reported a zinc-based metal–organic framework modified by carbon quantum dots (N–Zn-MOF/CQDs to reduce Cr(VI) in solar-driven photocatalytic fuel cell. $BiVO_4$/N–Zn-MOF/CQDs PFC system shows under optimized conditions that 100% Cr(VI) can be successfully removed within 120 min of visible-light illumination. In addition, the as-prepared material showed good stability even after five cycles.

Furthermore, Yang *et al.*[356] developed an acethydrazide functionalized Fe/Ni-MIL-53 MOF electrode. The material shows an important electrochemical reduction and good immobilization of Cr(VI).

To summarize, Table 7 presents effective MOFs for chromium adsorption from contaminated water.

4.2.6. Influential factors on heavy metal adsorption using MOFs. Xie *et al.*[373] synthesized nanocomposites GO-COOH/MOF-808 for heavy metals removal. In this work, pH is the influencing factor to reach the higher adsorption efficiency. They demonstrated that the adsorption equilibrium of heavy metal ions Pb(II), Cd(II), Co(II), Ni(II), and Cu(II) of the nanocomposites got to 20 min under condition of the initial concentration of 100 mg L^{-1} and pH value of 5.5. Hence, Pb(II), Cd(II), Co(II), Ni(II), and Cu(II) had higher adsorption efficiencies, which are 157.78 mg g^{-1}, 135.96 mg g^{-1}, 82.35 mg g^{-1}, 90.99 mg g^{-1}, and 91.49 mg g^{-1}, respectively. In the same way, Soltani *et al.*[374] prepared a functionalized $Ni_{50}Co_{50}$-layered double hydroxide/UiO-66-(Zr)-$(COOH)_2$ nanocomposite (LDH/MOF NC) as an effective adsorbent for removal of mercury cations from aqueous media. They showed that the adsorption performance of LDH/MOF NC for removal of Hg(II) and Ni(II) cations was influenced by some experimental factors. Accordingly, the optimum pH values were 3.0 for adsorption of Hg(II). The adsorption equilibrium for Hg(II) was almost achieved when the initial concentration was 100 mg L. Furthermore, the adsorption capacity increased sharply with increasing contact time from 1 min to 20 min. As result, They found that the maximum adsorption capacities based on the was 509.8 mg g^{-1} for Hg(II). Similarly, Li *et al.*[375] developed a composite material comprising Ti-MOF and chitosan, denoted as BD-MOF(Ti)@CS/Fe_3O_4 for the efficient adsorption of Pb(II) from aqueous solutions. The researchers found that the material has a high adsorption capacity of 99% (944 mg g^{-1}) between pH 3 and 6. Moreover, the adsorption efficiency reached 85% in 40 min. Besides, the material demonstrates noteworthy reusability, sustaining effective Pb(II) removal across five consecutive cycles in aqueous solutions. As follows, Chen *et al.*[376] synthesized a novel formic acid and amino modified MOFs referred to UIO-66-NH_2. They demonstrated that the pH at 2 of the solution was the decisive factor affecting the surface properties and adsorption capacity of adsorbent. In addition, form-UiO-66-NH_2 exhibited an excellent adsorption capacity of 338.98 mg g^{-1}. Along these lines, Ahmed *et al.*[377] prepared a citrate crosslinked chitosan composite sponge La-MOF@CSC as a novel adsorbent to eliminate Hg(II) from water. They demonstrated that the material sponge exhibited a maximum adsorption capacity for mercury at 765.22 mg g^{-1} with the optimal pH 5. Therefore, Nassef *et al.*[378] developed a unique Ag-MOF/chitosan composite sponge to remove Pb(II), Cu(II), and Cd(II) from aqueous solution. The material exhibited a high adsorption rates of 96.1% for Pb(II), 96.7% for Cu(II), and 95.95% for Cd(II),respectively. As a result, 0.25 g was chosen as the best option for increasing removal efficiency at pH 5 in contact for up to 60 min.

4.2.7. Selectivity of MOFs in complex systems. In this context, Lv, *et al.*[379] synthesized a series of amino-decorated

Table 7 Potential MOFs for chromium removal and reduction

Heavy metal	MOFs	pH	Adsorption capacity (mg g^{-1})	Contact time (min)	Ref.	Other adsorbents: Adsorption capacity (mg g^{-1})
Cr(VI)	ZIF-67-NZVI@ZD	5	226.5	180	357	Modified shrimp-based chitosan (20.37),[358] eggshell/poly pyrrole composites (175.5),[359] spoilt milk-derived adsorbent (640),[360] chromolaena odorata-derived magnetite nanoparticles (173.12),[361] nitrogen-functionalized graphene aerogel (458.24),[362] nanofibrillated cellulose (NFC)/chitosan (CS) aerogel (197.33),[363] pomegranate-peel-derived biochar (16.23)[364]
	Fe-MOFs-$Fe_{0.72}^{(0)}Fe_{2.28}^{(II)}C$	2	354.6	—	365	
	MIL-100(Fe)-nZVI@C	—	206.0	—	366	
	ZIF-67-Ni/Co-LDH	7	99.9	80	367	
	TMU-60	2–9	145.0	10	368	
	FIR-53	—	74.2	—	369	
	FIR-54	—	103	60		
	IL-MIL-100(Fe)	2	285.7	300	370	
	Non-protonated MOR-1	3	267	1	371	
	TMU-4	10	127	5	372	

MOFs as a universal sensing platform that demonstrated great potential for detecting and removing heavy metals with remarkable specificity and capability. In addition, MIL101-NH_2 demonstrated great adsorption ability and selectivity in removing Fe^{3+}, Cu^{2+} and Pb^{2+} from aqueous solution, and the adsorption capacities reached up to 3.5, 0.9 and 1.1 mM g^{-1}. Thus, Ji *et al.*[380] prepared a carboxyl adsorbent, MIL-121. The material demonstrated high adsorption selectivity for heavy metals at 10 000 mg L^{-1} of Na^+ by removal 99% of Cu^{2+} as well as unexpected easy regeneration (desorption > 99%) at low H^+ concentration (10–3.5–10–3.0 M). Similar high selectivity and easy regeneration were also satisfied with Pb^{2+} and removal of heavy metals remained 99% in 10 consecutive adsorption–desorption cycles. They showed the potential of MIL-121 for heavy metal wastewater treatment and provides mechanistic insight for developing adsorbents with high selective adsorption and easy regeneration. In other hand, Wu *et al.*[381] developed a high-efficient and easy-to-recover adsorbent a sulfur-functionalized MOF was incorporated into Ca-alginate/polyacrylic acid granulates (CPZ-SH) for the removal of Cu^{2+} and Cd^{2+} in water. They demonstrated that the material exhibited maximum adsorption capacities of 75.8 and 48.4 mg g^{-1} at 30 °C, and excellent adsorption reusability with Cu^{2+} and Cd^{2+} adsorption efficiencies over 96.0% and 85.1% after 10 cycles, respectively. Therefore, Nimbalkar *et al.*[382] synthesized a zirconium-based MOF employed for the adsorptive removal of and lead and cadmium from aqueous solution. They studied kinetics and isotherm to understand the nature and extent of adsorption. As result, they showed that adsorption capacities for cadmium and lead were found to be 37 and 100 mg g^{-1} respectively.

5. Ecologically friendly MOFs

Key considerations encompass the synthesis approach, stability of the resulting materials, as well as methods for regeneration and subsequent reuse.

Mahmoodi *et al.*[383] introduced an innovative adsorbent, a robust bionanocomposite eggshell membrane-zeolitic imidazolate framework ZIF-67@Fe_3O_4@ESM fabricated through an eco-friendly ultrasound-assisted method. Their study demonstrated that the Langmuir adsorption isotherm effectively described the equilibrium data, revealing a remarkable maximum adsorption capacity of 344.82 mg g^{-1} for Cu^{2+}. Kinetic investigations indicated that the pseudo-second order model aptly represented the experimental data for the simultaneous removal of heavy metal ions. Moreover, the magnetic properties of this adsorbent facilitated efficient separation through magnetization. Subsequent regeneration cycles demonstrated a gradual decline in efficiency, attributed to incomplete desorption and the occupation of active sites. Likewise, Guo *et al.*[384] constructed the Mg-MOF-74@CA composite an environmentally friendly metal–organic framework material. They found that the removal of Pb(II), Cd(II), and Cu(II) attained equilibriums at about 5 h. Furthermore, the removal of Pb(II), Cd(II), and Cu(II) were strongly influenced by solution pH, while almost independent of ionic strength and humic acid (HA). Thus, the maximum adsorption capacities of Pb(II), Cd(II), and Cu(II) at 298 K were 223.555, 160.033, and 74.349 mg g^{-1}, respectively. Whereas, Ji *et al.*[385] synthesized a unique magnetic Fe_3O_4/graphene oxide (GO) nanocomposite derived from MIL-100(Fe)/GO. They demonstrated that the as-prepared exhibited exceptional adsorption capacity for As(V) and possessed magnetic separation properties. Thus, compared with prepared MWCNTs/MIL-53(Fe)-15% adsorbent, the magnetic MIL-100(Fe)/1%GO-400 exhibited a striking increase in adsorption–desorption cycling performance of As(V) and a high recovery rate, which indicates a greater application potential in As removal in groundwater.

6. Conclusion and prospects

The promise of Metal–Organic Frameworks (MOFs) for removing heavy metals from contaminated water has been further confirmed by our research. We investigated the crucial influence of various parameters, including ligand selection, metal node composition, pore size, and surface area, on the adsorption performance of MOFs. Notably, Scanning Electron Microscopy (SEM) played a vital role in characterizing the morphology and pore structure of these synthesized MOFs, directly correlating these features to their adsorption capacities. Furthermore, we recognized the paramount importance of efficient desorption for the reusability of MOFs, exploring and evaluating suitable regeneration methods. This perspective solidifies the exceptional potential of MOFs for heavy metal removal. The demonstrated high surface areas, tunable pore structures, and tailorable functionalities of MOFs enable selective and efficient adsorption of specific metal ions. This research not only underscores the importance of careful MOF design but also highlights the critical role of characterization techniques like SEM and optimized regeneration strategies for achieving sustainable and reusable MOF-based solutions. Looking forward, MOF-based composites and hybrid materials offers exciting opportunities for further enhancing adsorption performance, recyclability, and scalability, paving the way for real-world implementation in large-scale water treatment applications. The ongoing exploration of MOFs and their applications in environmental remediation holds the key to a cleaner and safer environment. Thus, herein, we propose the following points for future development:

- Enhanced adsorption kinetics: future research can focus on improving the kinetics of heavy metal adsorption by optimizing MOF structures and synthesis methods. This could lead to faster and more efficient removal of heavy metals from contaminated water.
- Selective adsorption: investigating MOFs with even greater selectivity for specific heavy metal ions could lead to tailored adsorbents that are highly effective pollution scenarios.
- Hybrid and composite materials: exploring the development of MOF-based composite materials or hybrid systems that combine MOFs with other materials to enhance adsorption capacity, stability, and recyclability.
- Scale-up and industrial applications: transitioning from laboratory-scale experiments to larger-scale production and

application in real-world industrial settings. This involves addressing issues related to scalability, cost-effectiveness, and long-term stability.

• Waste management: research into the regeneration and safe disposal of spent MOF adsorbents, including recycling methods and potential secondary applications for the captured heavy metals.

• Environmental monitoring: developing MOF-based sensors for on-site environmental monitoring of heavy metal contamination, allowing for real-time detection and response.

• Green synthesis: developing environmentally friendly and sustainable methods for MOF synthesis, reducing the environmental footprint of the production process.

• Cost: reducing the cost for the synthesis of MOFs materials with a targeted surface area and crystallinity. This includes low energy consumption in synthesis strategies and low-cost reagents to avoid the use of organic solvents.

Author contributions

Sanaa Essalmi: writing the draft, data curation; formal analysis. Safia Lotfi: writing the draft, data curation; formal analysis. Amal BaQais: writing – review & editing. Mohamed Saadi: project administration; supervision and validation. Madjid Arab: writing – review & editing; project administration and supervision. Hassan Ait Ahsaine: writing the draft, project administration; supervision and validation.

Conflicts of interest

The authors declare that they have no known competing financial interests or personal relationships that could have appeared to influence the work reported in this paper.

Acknowledgements

We acknowledge the support from Mohammed V university and Toulon University.

References

1 J. Zhang, Soil Environmental Deterioration and Ecological Rehabilitation, *Study of Ecological Engineering of Human Settlements*, 2020, pp. 41–82.
2 A. Ebenstein, The Consequences of Industrialization: Evidence from Water Pollution and Digestive Cancers in China, *Rev. Econ. Stat.*, 2012, **94**, 186–201.
3 Q. Wu, H. Zhou, N. F. Y. Tam, Y. Tian, Y. Tan, S. Zhou, Q. Li, Y. Chen and J. Y. S. Leung, *Mar. Pollut. Bull.*, 2016, **104**, 153–161.
4 B. Sarker, K. N. Keya, F. I. Mahir, K. M. Nahiun, S. Shahida, R. A. Khan and A. History, *Sci. Rev.*, 2021, **7**, 32–41.
5 B. E. Channab, M. El Ouardi, S. E. Marrane, O. A. Layachi, A. El Idrissi, S. Farsad, D. Mazkad, A. BaQais, M. Lasri and H. Ait Ahsaine, *RSC Adv.*, 2023, **13**, 20150–20163.
6 M. El Ouardi, O. Ait Layachi, E. Amaterz, A. El Idrissi, A. Taoufyq, B. Bakiz, A. Benlhachemi, M. Arab, A. BaQais and H. Ait Ahsaine, *J. Photochem. Photobiol., A*, 2023, **444**, 115011.
7 A. Elaouni, M. El Ouardi, A. BaQais, M. Arab, M. Saadi and H. Ait Ahsaine, *RSC Adv.*, 2023, **13**, 17476–17494.
8 S. Roy, J. Darabdhara and M. Ahmaruzzaman, *RSC Sustainability*, 2023, **1**, 1952–1961.
9 S. Roy, J. Darabdhara and M. Ahmaruzzaman, *J. Hazard. Mater. Lett.*, 2024, **5**, 100094.
10 P. A. Kobielska, A. J. Howarth, O. K. Farha and S. Nayak, *Coord. Chem. Rev.*, 2018, **358**, 92–107.
11 J. Zhao, Z. Dang, M. Muddassir, S. Raza, A. Zhong, X. Wang and J. Jin, *Molecules*, 2023, **28**, 6848.
12 S. Roy, J. Darabdhara and M. Ahmaruzzaman, *J. Cleaner Prod.*, 2023, **430**, 139517.
13 *Inorganic Pollutants in Water*, ed. P. Borah, M. Kumar and P. Devi, Elsevier, 2020, pp. 17–31.
14 D. Mazkad, A. El Idrissi, S. E. Marrane, N. Eddine Lazar, M. El Ouardi, O. Dardari, B. E. Channab, O. Ait Layachi, S. Farsad, A. Baqais, E. M. Lotfi and H. Ait Ahsaine, *Colloids Surf., A*, 2024, **685**, 133172.
15 S. Lotfi, M. El Ouardi, H. Ait Ahsaine, V. Madigou, A. BaQais, A. Assani, M. Saadi and M. Arab, *Heliyon*, 2023, **9**, e17255.
16 M. El ouardi, A. El Idrissi, M. Arab, M. Zbair, H. Haspel, M. Saadi and H. Ait Ahsaine, *Int. J. Hydrogen Energy*, 2024, **51**, 1044–1067.
17 X. Qu, P. J. J. Alvarez and Q. Li, *Water Res.*, 2013, **47**, 3931–3946.
18 M. M. Pendergast and E. M. V. Hoek, *Energy Environ. Sci.*, 2011, **4**, 1946–1971.
19 V. K. Gupta, I. Ali, T. A. Saleh, A. Nayak and S. Agarwal, *RSC Adv.*, 2012, **2**, 6380–6388.
20 G. Crini and E. Lichtfouse, *Environ. Chem. Lett.*, 2019, **17**, 145–155.
21 A. Azimi, A. Azari, M. Rezakazemi and M. Ansarpour, *ChemBioEng Rev.*, 2017, **4**, 37–59.
22 W. S. Chai, Y. Cheun, P. Senthil Kumar, M. Mubashir, Z. Majeed, F. Banat, S.-H. Ho and P. Loke Show, *J. Clean. Prod.*, 2021, **296**, 126589.
23 S. Wadhawan, A. Jain, J. Nayyar and K. Mehta, *J. Water Process Eng.*, 2020, **33**, 101038.
24 E. Nazarzadeh Zare, A. Mudhoo, M. Ali Khan, M. Otero, Z. Muhammad Ali Bundhoo, C. Navarathna, M. Patel, A. Srivastava, C. U. Pittman Jr, T. Mlsna, D. Mohan, P. Makvandi and M. Sillanpää mikaetapiosillanpaa, *Environ. Chem. Lett.*, 2021, **19**, 17.
25 H. Darmokoesoemo, F. R. Setianingsih, T. W. L. C. Putranto and H. S. Kusuma, *Rasayan J. Chem*, 2016, **9**, 550–555.
26 E. P. Kuncoro, D. R. Mitha Isnadina, H. Darmokoesoemo, F. Dzembarahmatiny and H. S. Kusuma, *Data Brief*, 2018, **16**, 354–360.
27 S. Roy, J. Darabdhara and M. Ahmaruzzaman, *J. Cleaner Prod.*, 2023, **430**, 139517.
28 E. P. Kuncoro, D. R. M. Isnadina, H. Darmokoesoemo, O. R. Fauziah and H. S. Kusuma, *Data Brief*, 2018, **16**, 622–629.

29 E. P. Kuncoro, T. Soedarti, T. W. C. Putranto, H. Darmokoesoemo, N. R. Abadi and H. S. Kusuma, *Data Brief*, 2018, **16**, 908–913.
30 Y. A. B. Neolaka, A. A. P. Riwu, U. O. Aigbe, K. E. Ukhurebor, R. B. Onyancha, H. Darmokoesoemo and H. S. Kusuma, *Results Chem.*, 2023, **5**, 100711.
31 R. A. Khera, M. Iqbal, A. Ahmad, S. M. Hassan, A. Nazir, A. Kausar, H. S. Kusuma, J. Niasr, N. Masood, U. Younas, R. Nawaz and M. I. Khan, *Desalin. Water Treat.*, 2020, **201**, 289–300.
32 H. S. Kusuma, N. Illiyanasafa, D. E. C. Jaya, H. Darmokoesoemo and N. R. Putra, *Sustainable Chem. Pharm.*, 2024, **37**, 101346.
33 Y. A. B. Neolaka, Y. Lawa, J. Naat, A. C. Lalang, B. A. Widyaningrum, G. F. Ngasu, K. A. Niga, H. Darmokoesoemo, M. Iqbal and H. S. Kusuma, *Results Eng.*, 2023, **17**, 100824.
34 J. N. Naat, Y. A. B. Neolaka, T. Lapailaka, T. Rachmat Triandi, A. Sabarudin, H. Darmokoesoemo and H. S. Kusuma, *Rasayan J. Chem.*, 2021, **14**, 550–560.
35 J. Wang, J. Wan and C. Yu, *Coord. Chem. Rev.*, 2021, **432**, 213743.
36 C. P. Raptopoulou, *Materials*, 2021, **14**, 1–32.
37 E. Newton Augustus, A. Nimibofa, I. Azibaola Kesiye and W. Donbebe, *Am. J. Environ. Prot.*, 2017, **5**, 61–67.
38 M. A. Andrés, P. Fontaine, M. Goldmann, C. Serre, O. Roubeau and I. Gascón, *J. Colloid Interface Sci.*, 2021, **590**, 72–81.
39 P. Pachfule, R. Das, P. Poddar and R. Banerjee, *Cryst. Growth Des.*, 2011, **11**, 1215–1222.
40 C. Mckinstry, R. J. Cathcart, E. J. Cussen, A. J. Fletcher, S. V. Patwardhan and J. Sefcik, *J. Chem. Eng.*, 2016, **285**, 718–725.
41 S. S. Kaye, A. Dailly, O. M. Yaghi and J. R. Long, *J. Am. Chem. Soc.*, 2007, **129**, 14176–14177.
42 C. McKinstry, E. J. Cussen, A. J. Fletcher, S. V. Patwardhan and J. Sefcik, *Cryst. Growth Des.*, 2013, **13**, 5481–5486.
43 B. Zhang, Y. Luo, K. Kanyuck, N. Saenz, K. Reed, P. Zavalij, J. Mowery and G. Bauchan, *RSC Adv.*, 2018, **8**, 33059–33064.
44 K. Kamal, M. A. Bustam, M. Ismail, D. Grekov, A. M. Shariff and P. Pré, *Materials*, 2020, **13**, 2741.
45 V. H. Nguyen, L. Van Tan, T. Lee and T. D. Nguyen, *Sustainable Chem. Pharm.*, 2021, **20**, 100385.
46 A. K. Inge, M. Köppen, J. Su, M. Feyand, H. Xu, X. Zou, M. O'Keeffe and N. Stock, *J. Am. Chem. Soc.*, 2016, **138**, 1970–1976.
47 G. Wang, Q. Sun, Y. Liu, B. Huang, Y. Dai, X. Zhang, X. Qin, G. Wang, Y. Liu, B. Huang, X. Zhang, X. Qin, Q. Sun and Y. Dai, *Chem. –A Euro. J.*, 2015, **21**, 2364–2367.
48 L. Huang, H. Wang, J. Chen, Z. Wang, J. Sun, D. Zhao and Y. Yan, *Microporous Mesoporous Mater.*, 2003, **58**, 105–114.
49 J. Li, S. Cheng, Q. Zhao, P. Long and J. Dong, *Int. J. Hydrogen Energy*, 2009, **34**, 1377–1382.
50 R. R. Gonte, P. C. Deb and K. Balasubramanian, *J. Polym.*, 2013, **2013**, 1–8.
51 J. Hu, Y. Chen, H. Zhang, Z. Chen, Y. Ling, Y. Yang, X. Liu, Y. Jia and Y. Zhou, *Microporous Mesoporous Mater.*, 2021, **315**, 110900.
52 S. J. Doktycz and K. S. Suslick, Interparticle collisions driven by ultrasound, *Science (1979)*, 1990, **247**, 1067–1069.
53 K. S. Suslick, M. M. Fang, T. Hyeon and M. M. Mdleleni, *Sonochemistry and Sonoluminescence*, 1999, 291–320.
54 W. J. Son, J. Kim, J. Kim and W. S. Ahn, *Chem. Commun.*, 2008, 6336–6338.
55 M. Saidi, A. Benomara, M. Mokhtari and L. Boukli-Hacene, *React. Kinet., Mech. Catal.*, 2020, **131**, 1009–1021.
56 T. Wiwasuku, J. Othong, J. Boonmak, V. Ervithayasuporn and S. Youngme, *Dalton Trans.*, 2020, **49**, 10240–10249.
57 J. H. Lee, Y. Ahn and S. Y. Kwak, *ACS Omega*, 2022, **7**, 23213–23222.
58 H. V. Tran, H. T. M. Dang, L. T. Tran, C. Van Tran and C. D. Huynh, *Adv. Polym. Technol.*, 2020, **2020**, 6279278.
59 O. S. Bull, I. Bull, G. K. Amadi, C. Obaalologhi Odu and E. O. Okpa, *Orient. J. Chem.*, 2022, **38**, 490–516.
60 J. H. Lee, Y. Ahn and S. Y. Kwak, *ACS Omega*, 2022, **7**, 23213–23222.
61 J. A. Fuentes-García, J. Santoyo-Salzar, E. Rangel-Cortes, G. F. Goya, V. Cardozo-Mata and J. A. Pescador-Rojas, *Ultrason. Sonochem.*, 2021, **70**, 105274.
62 K. Yu, Y. Lee, J. Seo, K. Baek and W.-S. Ahn, *Microporous Mesoporous Mater.*, 2021, **316**, 110985.
63 T. Tsuruoka, S. Furukawa, Y. Takashima, K. Yoshida, S. Isoda and S. Kitagawa, *Angew. Chem., Int. Ed.*, 2009, **48**, 4739–4743.
64 A. Umemura, S. Diring, S. Furukawa, H. Uehara, T. Tsuruoka and S. Kitagawa, *J. Am. Chem. Soc.*, 2011, **133**, 15506–15513.
65 D. Braga, S. L. Giaffreda, M. Curzi, L. Maini, M. Polito and F. Grepioni, *J. Therm. Anal. Calorim.*, 2007, **90**, 115–123.
66 D. J. Tranchemontagne, J. R. Hunt and O. M. Yaghi, *Tetrahedron*, 2008, **64**, 8553–8557.
67 D. Chen, J. Zhao, P. Zhang and S. Dai, *Polyhedron*, 2019, **162**, 59–64.
68 M. Y. Masoomi, S. Beheshti and A. Morsali, *J. Mater. Chem. A*, 2014, **2**, 16863–16866.
69 M. Y. Masoomi, K. C. Stylianou, A. Morsali, P. Retailleau and D. Maspoch, *Cryst. Growth Des.*, 2014, **14**, 2092–2096.
70 A. Pichon, A. Lazuen-Garay and S. L. James, *CrystEngComm*, 2006, **8**, 211–214.
71 G. A. Bowmaker, *Chem. Commun.*, 2012, **49**, 334–348.
72 T. Friić and L. Fábián, *CrystEngComm*, 2009, **11**, 743–745.
73 D. Prochowicz, K. Sokołowski, I. Justyniak, A. Kornowicz, D. Fairen-Jimenez, T. Friščić and J. Lewiński, *Chem. Commun.*, 2015, **51**, 4032–4035.
74 P. J. Beldon, L. Fμbiμn, R. S. Stein, A. Thirumurugan, A. K. Cheetham, T. F. Friščić*, P. J. Beldon, T. Friščicfriščić, L. Fμbiμn, R. S. Stein and A. K. Cheetham, *Angew. Chem.*, 2010, **122**, 9834–9837.
75 C.-A. Tao, J.-F. Wang, C.-A. Tao and J.-F. Wang, *Crystals*, 2021, **11**, 15.
76 P. A. Julien, K. Užarević, A. D. Katsenis, S. A. J. Kimber, T. Wang, O. K. Farha, Y. Zhang, J. Casaban,

L. S. Germann, M. Etter, R. E. Dinnebier, S. L. James, I. Halasz and T. Friščić, *J. Am. Chem. Soc.*, 2016, **138**, 2929–2932.
77 M. Y. Masoomi, A. Morsali and P. C. Junk, *CrystEngComm*, 2014, **17**, 686–692.
78 Z. Wang, Z. Li, M. Ng and P. J. Milner, *Dalton Trans.*, 2020, **49**, 16238–16244.
79 J. Beamish-Cook, K. Shankland, C. A. Murray and P. Vaqueiro, *Cryst. Growth Des.*, 2021, **21**, 3055.
80 C. Dey, T. Kundu, B. P. Biswal, A. Mallick and R. Banerjee, *Acta Crystallogr., Sect. B: Struct. Sci., Cryst. Eng. Mater.*, 2014, **70**, 3–10.
81 H. Al-Kutubi, J. Gascon, E. J. R. Sudhölter and L. Rassaei, *ChemElectroChem*, 2015, **2**, 462–474.
82 H. M. Yang, X. Liu, X. L. Song, T. L. Yang, Z. H. Liang and C. M. Fan, *Trans. Nonferrous Met. Soc. China*, 2015, **25**, 3987–3994.
83 D. Liu, J. J. Purewal, J. Yang, A. Sudik, S. Maurer, U. Mueller, J. Ni and D. J. Siegel, *Int. J. Hydrogen Energy*, 2012, **37**, 6109–6117.
84 M. Moreno, M. Montanino, M. Carewska, G. B. Appetecchi, S. Jeremias and S. Passerini, *Electrochim. Acta*, 2013, **99**, 108–116.
85 H. Y. Liu, H. Wu, J. Yang, Y. Y. Liu, B. Liu, Y. Y. Liu and J. F. Ma, *Cryst. Growth Des.*, 2011, **11**, 2920–2927.
86 J. Z. Wei, F. X. Gong, X. J. Sun, Y. Li, T. Zhang, X. J. Zhao and F. M. Zhang, *Inorg. Chem.*, 2019, **58**, 6742–6747.
87 A. Martinez Joaristi, J. Juan-Alcañiz, P. Serra-Crespo, F. Kapteijn and J. Gascon, *Cryst. Growth Des.*, 2012, **12**, 3489–3498.
88 H. Furukawa and O. M. Yaghi, *J. Am. Chem. Soc.*, 2009, **131**, 8875–8883.
89 R.-B. Lin, S. Xiang, W. Zhou and B. Chen, *Chem*, 2020, **6**, 337–363.
90 H. Furukawa, K. Cordova, M. O'Keeffe and O. M. Yaghi, *Science*, 2013, **341**, 6149.
91 K. S. Park, Z. Ni, A. P. Côté, J. Y. Choi, R. Huang, F. J. Uribe-Romo, H. K. Chae, M. O'Keeffe and O. M. Yaghi, *Proc. Natl. Acad. Sci. U. S. A.*, 2006, **103**, 10186–10191.
92 M. J. Kalmutzki, N. Hanikel and O. M. Yaghi, *Sci. Adv.*, 2018, 4.
93 H. Furukawa, N. Ko, Y. B. Go, N. Aratani, S. B. Choi, E. Choi, A. Ö. Yazaydin, R. Q. Snurr, M. O'Keeffe, J. Kim and O. M. Yaghi, *Science (1979)*, 2010, **329**, 424–428.
94 O. K. Farha, I. Eryazici, N. C. Jeong, B. G. Hauser, C. E. Wilmer, A. A. Sarjeant, R. Q. Snurr, S. T. Nguyen, A. Ö. Yazaydin and J. T. Hupp, *J. Am. Chem. Soc.*, 2012, **134**, 15016–15021.
95 M. Y. Masoomi, A. Morsali, A. Dhakshinamoorthy and H. Garcia, *Angew. Chemie*, 2019, **131**, 15330–15347.
96 S. Chaemchuen, N. A. Kabir, K. Zhou and F. Verpoort, *Chem. Soc. Rev.*, 2013, **42**, 9304–9332.
97 H. Li, K. Wang, Y. Sun, C. T. Lollar, J. Li and H. C. Zhou, *Mater. Today*, 2018, **21**, 108–121.
98 H. Li, L. Li, R. B. Lin, W. Zhou, Z. Zhang, S. Xiang and B. Chen, *EnergyChem*, 2019, **1**, 100006.
99 X. Zhao, Y. Wang, D. S. Li, X. Bu and P. Feng, *Adv. Mater.*, 2018, **30**, 1705189.
100 D. H. Hong, H. S. Shim, J. Ha and H. R. Moon, *Bull. Korean Chem. Soc.*, 2021, **42**, 956–969.
101 J. D. Xiao and H. L. Jiang, *Acc. Chem. Res.*, 2019, **52**, 356–366.
102 H. Wang, *Nano Res.*, 2021, **15**, 2834–2854.
103 H. Cai, Y. L. Huang and D. Li, *Coord. Chem. Rev.*, 2019, **378**, 207–221.
104 M. Shyngys, J. Ren, X. Liang, J. Miao, A. Blocki and S. Beyer, *Front. bioeng. biotechnol.*, 2021, **9**, 603608.
105 P. Kumar, A. Deep and K. H. Kim, *TrAC, Trends Anal. Chem.*, 2015, **73**, 39–53.
106 E. A. Dolgopolova, A. M. Rice, C. R. Martin and N. B. Shustova, *Chem. Soc. Rev.*, 2018, **47**, 4710–4728.
107 M. Sabo, A. Henschel, H. Fröde, E. Klemm and S. Kaskel, *J. Mater. Chem.*, 2007, **17**, 3827–3832.
108 X. W. Liu, Y. M. Gu, T. J. Sun, Y. Guo, X. L. Wei, S. S. Zhao and S. D. Wang, *Ind. Eng. Chem. Res.*, 2019, **58**, 20392–20400.
109 W. J. Koros and C. Zhang, *Nat. Mater.*, 2017, **16**, 289–297.
110 S. Chaemchuen, N. A. Kabir, K. Zhou and F. Verpoort, *Chem. Soc. Rev.*, 2013, **42**, 9304–9332.
111 Z. Raji, A. Karim, A. Karam and S. Khalloufi, *Waste*, 2023, **1**, 775–805.
112 N. A. A. Qasem, R. H. Mohammed and D. U. Lawal, *NPJ Clean Water*, 2021, **4**, 52.
113 P. Pourhakkak, A. Taghizadeh, M. Taghizadeh, M. Ghaedi and S. Haghdoust, *Interface Sci. Technol.*, 2021, **33**, 1–70.
114 N. Manousi, D. A. Giannakoudakis, E. Rosenberg and G. A. Zachariadis, *Molecules*, 2019, **24**, 4605.
115 M. R. Momeni, Z. Zhang, D. Dell'Angelo and F. A. Shakib, *Phys. Chem. Chem. Phys.*, 2021, **23**, 3135–3143.
116 Z. Raji, A. Karim, A. Karam and S. Khalloufi, *Waste*, 2023, **1**, 775–805.
117 T. S. Vo, M. M. Hossain, H. M. Jeong and K. Kim, *Nano Convergence*, 2020, **7**, 36.
118 D. Wang and T. Li, *Acc. Chem. Res.*, 2023, **56**, 462–474.
119 D. Wu, P. F. Zhang, G. P. Yang, L. Hou, W. Y. Zhang, Y. F. Han, P. Liu and Y. Y. Wang, *Coord. Chem. Rev.*, 2021, **434**, 213709.
120 B. Han and A. Chakraborty, *Appl. Therm. Eng.*, 2023, **218**, 119365.
121 Y. Liang, X. Yang, X. Wang, Z. J. Guan, H. Xing and Y. Fang, *Nat. Commun.*, 2023, **14**, 1–14.
122 X. Li, K. Chen, R. Guo and Z. Wei, *Chem. Rev.*, 2023, **123**, 10432–10467.
123 C. Wang, C. Xiong, Y. He, C. Yang, X. Li, J. Zheng and S. Wang, *Chem. Eng. J.*, 2021, **415**, 128923.
124 M. Cai, G. Chen, L. Qin, C. Qu, X. Dong, J. Ni and X. Yin, *Pharmaceutics*, 2020, **12**, 232.
125 O. M. Yaghi, N. W. Ockwig, H. K. Chae, M. Eddaoudi and J. Kim, *Nature*, 2003, **423**, 705–714.
126 K. L. B. Solis, Y. H. Kwon, M. H. Kim, H. R. An, C. Jeon and Y. Hong, *Chemosphere*, 2020, **238**, 124656.
127 S. Dhaka, R. Kumar, A. Deep, M. B. Kurade, S. W. Ji and B. H. Jeon, *Coord. Chem. Rev.*, 2019, **380**, 330–352.

128 A. Tchinsa, M. F. Hossain, T. Wang and Y. Zhou, *Chemosphere*, 2021, **284**, 131393.
129 C. A. Trickett, A. Helal, B. A. Al-Maythalony, Z. H. Yamani, K. E. Cordova and O. M. Yaghi, *Nat. Rev. Mater.*, 2017, **2**, 17045.
130 I. Skarmoutsos, Y. Belmabkhout, K. Adil, M. Eddaoudi and G. Maurin, *J. Phys. Chem. C*, 2017, **121**, 27462–27472.
131 Z. Raji, A. Karim, A. Karam and S. Khalloufi, *Waste*, 2023, **1**, 775–805.
132 M. Musah, Y. Azeh, J. Mathew, M. Umar, Z. Abdulhamid and A. Muhammad, *Caliphate Journal of Science and Technology*, 2022, **4**, 20–26.
133 É. C. Lima, M. A. Adebayo and F. M. Machado, *Carbon Nanostruct.*, 2015, pp. 33–69.
134 S. T. Nipa, N. R. Shefa, S. Parvin, M. A. Khatun, M. J. Alam, S. Chowdhury, M. A. R. Khan, S. M. A. Z. Shawon, B. K. Biswas and M. W. Rahman, *Results Eng.*, 2023, **17**, 100857.
135 M. Vigdorowitsch, A. Pchelintsev, L. Tsygankova and E. Tanygina, *Appl. Sci.*, 2021, **11**, 8078.
136 A. El Ghali, M. H. V. Baouab and M. S. Roudesli, *Fibers Polym.*, 2013, **14**, 65–75.
137 R. Ragadhita and A. B. D. Nandiyanto, *Indones. J. Sci. Technol.*, 2021, **6**, 205–234.
138 L. Parida and T. N Patel, *Environ. Monit. Assess.*, 2023, **195**, 766.
139 N. A. A. Qasem, R. H. Mohammed and D. U. Lawal, *npj Clean Water*, 2021, **4**, 1–15.
140 Z. Li, L. Wang, L. Qin, C. Lai, Z. Wang, M. Zhou, L. Xiao, S. Liu and M. Zhang, *Chemosphere*, 2021, **285**, 131432.
141 C. Li, K. Zhou, W. Qin, C. Tian, M. Qi, X. Yan and W. Han, *Soil Sediment Contam.: Int. J.*, 2019, **28**, 380–394.
142 A. Zwolak, M. Sarzyńska, E. Szpyrka and K. Stawarczyk, *Water, Air, Soil Pollut.*, 2019, **230**, 1–9.
143 G. Qin, Z. Niu, J. Yu, Z. Li, J. Ma and P. Xiang, *Chemosphere*, 2021, **267**, 129205.
144 WHO, General Condition of Drinking Water in Nepal, *Korean Society of Water Sciences Conference*, 2013, vol. 2013, pp. 182–183.
145 WHO, Progress on drinking-water, sanitation and hygiene: 2017 update and SDG baselines, 116, ISBN: 978-92-4-151289-3.
146 EPA, National primary drinking water regulations: Long Term 1 Enhanced Surface Water Treatment Rule, *Final rule*, 2002, vol. 67, pp. 1811–1844.
147 I. Balan, M. Shivakumar and P. M. Kumar, *Chron. Young Sci.*, 2012, **3**, 146.
148 J. Brinkel, M. H. Khan and A. Kraemer, *Int. J. Environ. Res. Public Health*, 2009, **6**, 1609–1619.
149 E. H. Syed, K. C. Poudel, K. Sakisaka, J. Yasuoka, H. Ahsan and M. Jimba, *J. Health Popul. Nutr.*, 2012, **30**, 262.
150 G. Sun, Arsenic contamination and arsenicosis in China, *Toxicol. Appl. Pharmacol.*, 2004, **198**, 268–271.
151 P. H. Chen, Y. C. Ko, Y. H. Yang, Y. C. Lin, T. Y. Shieh, C. H. Chen and C. C. Tsai, *Oral Oncol.*, 2004, **40**, 847–855.
152 L. Chen, L. Lei, T. Jin, M. Nordberg and G. F. Nordberg, *Diabetes Care*, 2006, **29**, 2682–2687.
153 Y. Chen, F. Parvez, M. Gamble, T. Islam, A. Ahmed, M. Argos, J. H. Graziano and H. Ahsan, *Toxicol. Appl. Pharmacol.*, 2009, **239**, 184–192.
154 Y. Chen, J. H. Graziano, F. Parvez, M. Liu, V. Slavkovich, T. Kalra, M. Argos, T. Islam, A. Ahmed, M. Rakibuz-Zaman, R. Hasan, G. Sarwar, D. Levy, A. Van Geen and H. Ahsan, *Toxicol. Appl. Pharmacol.*, 2009, **239**, 184–192.
155 C. H. Wang, C. K. Hsiao, C. L. Chen, L. I. Hsu, H. Y. Chiou, S. Y. Chen, Y. M. Hsueh, M. M. Wu and C. J. Chen, *Toxicol. Appl. Pharmacol.*, 2007, **222**, 315–326.
156 R. Hubaux, D. D. Becker-Santos, K. S. S. Enfield, D. Rowbotham, S. Lam, W. L. Lam and V. D. Martinez, *Mol. Cancer*, 2013, **12**, 1–11.
157 K. Salnikow and A. Zhitkovich, *Chem. Res. Toxicol.*, 2008, **21**, 28–44.
158 L. F. Jiang, T. M. Yao, Z. L. Zhu, C. Wang and L. N. Ji, *Biochim. Biophys. Acta, Proteins Proteomics*, 2007, **1774**, 1414–1421.
159 L. Hellström, C. G. Elinder, B. Dahlberg, M. Lundberg, L. Järup, B. Persson and O. Axelson, *Am. J. Kidney Dis.*, 2001, **38**, 1001–1008.
160 C. Nagata, Y. Nagao, C. Shibuya, Y. Kashiki and H. Shimizu, *Cancer Epidemiol., Biomarkers Prev.*, 2005, **14**, 705–708.
161 P. Garcia-Morales, M. Saceda, N. Kenney, N. Kim, D. S Salomon, M. M Gottardis, H. B Solomon, P. F Sholler, V. C. Jordan and M. B. Martin, *J. Biol. Chem.*, 1994, **269**, 16896.
162 R. Schutte, T. S. Nawrot, T. Richart, L. Thijs, D. Vanderschueren, T. Kuznetsova, E. Van Hecks, H. A. Roels and J. A. Staessen, *Environ. Health Perspect.*, 2008, **116**, 777–783.
163 G. G. Schwartz, D. Il'Yasova and A. Ivanova, *Diabetes Care*, 2003, **26**, 468–470.
164 M. Hadavifar, N. Bahramifar, H. Younesi, M. Rastakhiz, Q. Li, J. Yu and E. Eftekhari, *J. Taiwan Inst. Chem. Eng.*, 2016, **67**, 397–405.
165 R. A. Shih, H. Hu, M. G. Weisskopf and B. S. Schwartz, *Environ. Health Perspect.*, 2007, **115**, 483–492.
166 B. S. Schwartz, W. F. Stewart, K. I. Bolla, D. Simon, K. Bandeen-Roche, B. Gordon, J. M. Links and A. C. Todd, *Neurology*, 2000, **55**, 1144–1150.
167 A. G. Vij, *Al Ameen J. Med. Sci.*, 2009, **2**, 27–36.
168 A. Navas-Acien, E. Guallar, E. K. Silbergeld and S. J. Rothenberg, *Environ. Health Perspect.*, 2007, **115**, 472–482.
169 S. M. Levin and M. Goldberg, *Am. J. Ind. Med.*, 2000, **37**, 23–43.
170 A. Anttila, P. Apostoli, J. A. Bond, L. Gerhardsson, B. L. Gulson, A. Hartwig, P. Hoet, M. Ikeda, E. K. Jaffe, P. J. Landrigan, L. Levy, H. L. Needleman, E. J. O'Flaherty, S. Olin, J. H. Olsen, T. G. Rossman, T. Sakai, X. Shen, T. Sorahan, K. Steenland, F. W. Sunderman, T. M. Tavares, R. D. Tripathi and M. P. Waalkes, *IARC monographs on the evaluation of carcinogenic risks to humans: Inorganic and organic lead compounds*, World Health Organization International Agency for Research on Cancer, 2006, vol. 87.

171 J. Hu, C. Chen, X. Zhu and X. Wang, *J. Hazard. Mater.*, 2009, **162**, 1542–1550.
172 P. Miretzky and A. F. Cirelli, *J. Hazard. Mater.*, 2010, **180**, 1–19.
173 R. J. Lifset, M. J. Eckelman, E. M. Harper, Z. Hausfather and G. Urbina, *Sci. Total Environ.*, 2012, **417–418**, 138–147.
174 S. Kanumakala, A. Boneh and M. Zacharin, *J. Inherited Metab. Dis*, 2002, **25**, 391–398.
175 G. S. Simate, N. Maledi, A. Ochieng, S. Ndlovu, J. Zhang and L. F. Walubita, *J. Environ. Chem. Eng.*, 2016, **4**, 2291–2312.
176 S. Rajendran, T. A. K. Priya, K. S. Khoo, T. K. A. Hoang, H. S. Ng, H. S. H. Munawaroh, C. Karaman, Y. Orooji and P. L. Show, *Chemosphere*, 2022, **287**, 132369.
177 C. Zamora-Ledezma, D. Negrete-Bolagay, F. Figueroa, E. Zamora-Ledezma, M. Ni, F. Alexis and V. H. Guerrero, *Environ. Technol. Innovation*, 2021, **22**, 101504.
178 M. J. Manos and M. G. Kanatzidis, *J. Am. Chem. Soc.*, 2012, **134**, 16441–16446.
179 S. Yang, J. Hu, C. Chen, D. Shao and X. Wang, *Environ. Sci. Technol.*, 2011, **45**, 3621–3627.
180 J. Li, C. Chen, R. Zhang and X. Wang, *Sci. China: Chem*, 2016, **59**, 150–158.
181 S. S. Fiyadh, M. A. AlSaadi, W. Z. Jaafar, M. K. AlOmar, S. S. Fayaed, N. S. Mohd, L. S. Hin and A. El-Shafie, *J. Cleaner Prod.*, 2019, **230**, 783–793.
182 N. Abdollahi, G. Moussavi and S. Giannakis, *J. Environ. Chem. Eng.*, 2022, **10**, 107394.
183 H. Park, L. Wang and J. H. Yun, *J. Hazard. Mater.*, 2021, **416**, 125853.
184 S. Mohan and R. Gandhimathi, *J. Hazard. Mater.*, 2009, **169**, 351–359.
185 S. Wang, M. Soudi, L. Li and Z. H. Zhu, *J. Hazard. Mater.*, 2006, **133**, 243–251.
186 G. Sheng, S. Yang, J. Sheng, J. Hu, X. Tan and X. Wang, *Environ. Sci. Technol.*, 2011, **45**, 7718–7726.
187 Y. Sun, R. Zhang, C. Ding, X. Wang, W. Cheng, C. Chen and X. Wang, *Geochim. Cosmochim. Acta*, 2016, **180**, 51–65.
188 M. K. Uddin, *Chem. Eng. J.*, 2017, **308**, 438–462.
189 Y. Liu, L. Hu, B. Tan, J. Li, X. Gao, Y. He, X. Du, W. Zhang and W. Wang, *Int. J. Biol. Macromol.*, 2019, **141**, 738–746.
190 S. S. Ahluwalia and D. Goyal, *Bioresour. Technol.*, 2007, **98**, 2243–2257.
191 Z. Li, L. Wang, L. Qin, C. Lai, Z. Wang, M. Zhou, L. Xiao, S. Liu and M. Zhang, *Chemosphere*, 2021, **285**, 131432.
192 O. A. Oyewo, E. E. Elemike, D. C. Onwudiwe and M. S. Onyango, *Int. J. Biol. Macromol.*, 2020, **164**, 2477–2496.
193 N. Elboughdiri, *Cogent Eng.*, 2024, DOI: **10.1080/23311916.2020.1782623**.
194 P. Hadi, M. H. To, C. W. Hui, C. S. K. Lin and G. McKay, *Water Res.*, 2015, **73**, 37–55.
195 M. Mariana, A. K. Abdul, E. M. Mistar, E. B. Yahya, T. Alfatah, M. Danish and M. Amayreh, *J. Water Proc. engineering*, 2021, **43**, 102221.
196 A. Modak, P. Bhanja, M. Selvaraj and A. Bhaumik, *Environ. Sci.: Nano*, 2020, **7**, 2887–2923.
197 *Nano-Enabled Technologies for Water Remediation*, ed. M. Sonker, N. Shreyash, S. K. Tiwary, W. G. Shim and M. S. Balathanigaimani, Elsevier, 2022, pp. 515–553.
198 T. L. Tan, P. A. Krusnamurthy, H. Nakajima and S. A. Rashid, *RSC Adv.*, 2020, **10**, 18740–18752.
199 W. Zhang, H. Duo, S. Li, Y. An, Z. Chen, Z. Liu, Y. Ren, S. Wang, X. Zhang and X. Wang, *Colloid Interface Sci. Commun.*, 2020, **38**, 100308.
200 M. Sprynskyy, B. Buszewski, A. P. Terzyk and J. Namieśnik, *J. Colloid Interface Sci.*, 2006, **304**, 21–28.
201 C. Pelekani and V. L. Snoeyink, *Water Res.*, 1999, **33**, 1209–1219.
202 G. Oliveux, L. O. Dandy and G. A. Leeke, *Prog. Mater. Sci.*, 2015, **72**, 61–99.
203 S. A. Razzak, M. O. Faruque, Z. Alsheikh, L. Alsheikhmohamad, D. Alkuroud, A. Alfayez, S. M. Z. Hossain and M. M. Hossain, *Environ. Adv.*, 2022, **7**, 100168.
204 Y. Chen, X. Bai and Z. Ye, *Nanomaterials*, 2020, **10**, 1–23.
205 S. Lata, P. K. Singh and S. R. Samadder, *Int. J. Environ. Sci. Technol.*, 2015, **12**, 1461–1478.
206 X. Zhao, X. Yu, X. Wang, S. Lai, Y. Sun and D. Yang, *Chem. Eng. J.*, 2021, **407**, 127221.
207 P. A. Julien, C. Mottillo and T. Friščić, *Green Chem.*, 2017, **19**, 2729–2747.
208 C. H. Hendon, A. J. Rieth, M. D. Korzyński and M. Dincă, *ACS Cent. Sci.*, 2017, **3**, 554–563.
209 S. Kumar, S. Jain, M. Nehra, N. Dilbaghi, G. Marrazza and K. H. Kim, *Coord. Chem. Rev.*, 2020, **420**, 213407.
210 X. Zhao, S. Liu, Z. Tang, H. Niu, Y. Cai, W. Meng, F. Wu and J. P. Giesy, *Sci. Rep.*, 2015, **5**, 1–10.
211 G. Liu, L. Li, D. Xu, X. Huang, X. Xu, S. Zheng, Y. Zhang and H. Lin, *Carbohydr. Polym.*, 2017, **175**, 584–591.
212 Z. Li, L. Wang, L. Qin, C. Lai, Z. Wang, M. Zhou, L. Xiao, S. Liu and M. Zhang, *Chemosphere*, 2021, **285**, 131432.
213 E. Dhivya, D. Magadevan, Y. Palguna, T. Mishra and N. Aman, *J. Environ. Chem. Eng.*, 2019, **7**, 103240.
214 R. Ghanbari, E. Nazarzadeh Zare, A. C. Paiva-Santos and N. Rabiee, *Chemosphere*, 2023, **311**, 137191.
215 N. D. Rudd, H. Wang, E. M. A. Fuentes-Fernandez, S. J. Teat, F. Chen, G. Hall, Y. J. Chabal and J. Li, *ACS Appl. Mater. Interfaces*, 2016, **8**, 30294–30303.
216 P. Zhou, J. Wu, S. Tian, S. Li, Y. He, S. Zhang and T. Sun, *Prog. Org. Coat.*, 2024, **187**, 108115.
217 J. Zhao, J. He, L. Liu, S. Shi, H. Guo, L. Xie, X. Chai, K. Xu, G. Du and L. Zhang, *Sep. Purif. Technol.*, 2023, **327**, 124942.
218 Y. Zhang, L. Zhang, N. Wang, C. Feng, Q. Zhang, J. Yu, Y. Jiao, Y. Xu and J. Chen, *J. Environ. Chem. Eng.*, 2023, **11**, 111413.
219 S. Zhang, J. Ding, D. Tian, W. Su, F. Liu, Q. Li and M. Lu, *J. Mol. Struct.*, 2024, **1300**, 137313.
220 F. U. Haider, C. Liqun, J. A. Coulter, S. A. Cheema, J. Wu, R. Zhang, M. Wenjun and M. Farooq, *Ecotoxicol. Environ. Saf.*, 2021, **211**, 111887.
221 T. S. Nawrot, J. A. Staessen, H. A. Roels, E. Munters, A. Cuypers, T. Richart, A. Ruttens, K. Smeets, H. Clijsters and J. Vangronsveld, *BioMetals*, 2010, **23**, 769–782.

222 M. Mezynska and M. M. Brzóska, *Environ. Sci. Pollut. Res.*, 2017, **25**, 3211–3232.
223 Z. Yuan, T. Luo, X. Liu, H. Hua, Y. Zhuang, X. Zhang, L. Zhang, Y. Zhang, W. Xu and J. Ren, *Sci. Total Environ.*, 2019, **676**, 87–96.
224 J. M. R. Antoine, L. A. H. Fung and C. N. Grant, *Toxicol. Rep.*, 2017, **4**, 181–187.
225 H. Karababa, M. Atasoy, D. Yildiz, İ. Kula and M. Tuzen, *ACS Omega*, 2023, **8**, 7063–7069.
226 A. Giovanna Niño-Savala, Z. Zhuang, A. Fangmeier, A. Tang and X. Liu, *Front. Agric. Sci. Eng.*, 2019, **6**, DOI: **10.15302/J-FASE-2019273**.
227 J. Zhang, Z. Xiong, C. Li and C. Wu, *J. Mol. Liq.*, 2016, **221**, 43–50.
228 M. Roushani, Z. Saedi and Y. M. Baghelani, *Environ. Nanotechnol., Monit. Manage.*, 2017, **7**, 89–96.
229 S. Jamshidifard, S. Koushkbaghi, S. Hosseini, S. Rezaei, A. Karamipour, A. Jafari rad and M. Irani, *J. Hazard. Mater.*, 2019, **368**, 10–20.
230 E. Binaeian, S. Maleki, N. Motaghedi and M. Arjmandi, *Sep. Sci. Technol.*, 2020, **55**, 2713–2728.
231 C. Liu, P. Wang, X. Liu, X. Yi, D. Liu and Z. Zhou, *Chem.–Asian J.*, 2019, **14**, 261–268.
232 A. S. Yusuff, L. T. Popoola and E. O. Babatunde, *Appl. Water Sci.*, 2019, **9**, 1–11.
233 M. E. Mahmoud, M. F. Amira, S. M. Seleim and A. K. Mohamed, *J. Hazard. Mater.*, 2020, **381**, 120979.
234 W. S. Abo El-Yazeed, Y. G. Abou El-Reash, L. A. Elatwy and A. I. Ahmed, *J. Taiwan Inst. Chem. Eng.*, 2020, **114**, 199–210.
235 Y. Kim, K. Kim, H. H. Eom, X. Su and J. W. Lee, *Chem. Eng. J.*, 2021, **421**, 129765.
236 S. Singh, S. Kaushal, J. Kaur, G. Kaur, S. K. Mittal and P. P. Singh, *Chemosphere*, 2021, **272**, 129648.
237 F. Ahmadijokani, S. Tajahmadi, A. Bahi, H. Molavi, M. Rezakazemi, F. Ko, T. M. Aminabhavi and M. Arjmand, *Chemosphere*, 2021, **264**, 128466.
238 A. S. Abdelmoaty, S. T. El-Wakeel, N. Fathy and A. A. Hanna, *J. Inorg. Organomet. Polym. Mater.*, 2022, **32**, 2557–2567.
239 S. Gul, Z. Ahmad, M. Asma, M. Ahmad, K. Rehan, M. Munir, A. A. Bazmi, H. M. Ali, Y. Mazroua, M. A. Salem, M. S. Akhtar, M. S. Khan, L. F. Chuah and S. Asif, *Chemosphere*, 2022, **307**, 135633.
240 A. F. Abdel-Magied, H. N. Abdelhamid, R. M. Ashour, L. Fu, M. Dowaidar, W. Xia and K. Forsberg, *J. Environ. Chem. Eng.*, 2022, **10**, 107467.
241 J. E. Efome, D. Rana, T. Matsuura and C. Q. Lan, *ACS Appl. Mater. Interfaces*, 2018, **10**, 18619–18629.
242 B. F. M. L. Gomes, C. M. B. de Araújo, B. F. do Nascimento, E. M. P. L. de Freire, M. A. Da Motta Sobrinho and M. N. Carvalho, *Environ. Sci. Pollut. Res.*, 2022, **29**, 17358–17372.
243 J. Anwar, U. Shafique, Waheed-uz-Zaman, M. Salman, A. Dar and S. Anwar, *Bioresour. Technol.*, 2010, **101**, 1752–1755.
244 G. Murithi, C. O. Onindo, E. W. Wambu and G. K. Muthakia, *BioRes*, 2014, **9**(2), 3613–3631.
245 J. Qu, X. Meng, X. Jiang, H. You, P. Wang and X. Ye, *J. Cleaner Prod.*, 2018, **183**, 880–886.
246 Y. Li, M. Zhou, G. I. N. Waterhouse, J. Sun, W. Shi and S. Ai, *Environ. Sci. Pollut. Res.*, 2021, **28**, 5149–5157.
247 A. A. Bhutto, J. A. Baig, S. uddin, T. G. Kazi, R. Sierra-Alvarez, K. Akhtar, S. Perveen, H. I. Afridi, H. E. Ali, A. Hol and S. Samejo, *Ceram. Int.*, 2023, **49**, 14615–14623.
248 R. Zhao, B. Wang, P. Wu, Q. Feng, M. Chen, X. Zhang and S. Wang, *Sci. Total Environ.*, 2023, **894**, 164810.
249 F. Ahmadijokani, S. Tajahmadi, A. Bahi, H. Molavi, M. Rezakazemi, F. Ko, T. M. Aminabhavi and M. Arjmand, *Chemosphere*, 2021, **264**, 128466.
250 S. E. Moradi, A. M. H. Shabani, S. Dadfarnia and S. Emami, *Anal. Methods*, 2016, **8**, 6337–6346.
251 F. A. Elaiwi and A. Sirkecioglu, *Sep. Sci. Technol.*, 2020, **55**, 3362–3374.
252 K. Wang, J. Gu and N. Yin, *Ind. Eng. Chem. Res.*, 2017, **56**, 1880–1887.
253 S. Ul Mehdi and K. Aravamudan, *Mater. Today: Proc.*, 2022, **61**, 487–497.
254 M. E. Mahmoud, M. F. Amira, S. M. Seleim and A. K. Mohamed, *J. Hazard. Mater.*, 2020, **381**, 120979.
255 M. Roushani, Z. Saedi and Y. M. Baghelani, *Environ. Nanotechnol., Monit. Manage.*, 2017, **7**, 89–96.
256 J. C. Ng, J. Wang and A. Shraim, *Chemosphere*, 2003, **52**, 1353–1359.
257 M. F. Naujokas, B. Anderson, H. Ahsan, H. Vasken Aposhian, J. H. Graziano, C. Thompson and W. A. Suk, *Environ. Health Perspect.*, 2013, **121**, 295–302.
258 I. Palma-Lara, M. Martínez-Castillo, J. C. Quintana-Pérez, M. G. Arellano-Mendoza, F. Tamay-Cach, O. L. Valenzuela-Limón, E. A. García-Montalvo and A. Hernández-Zavala, *Regul. Toxicol. Pharmacol.*, 2020, **110**, 104539.
259 J. Brinkel, M. H. Khan and A. Kraemer, *Int. J. Environ. Res. Public Health*, 2009, **6**, 1609–1619.
260 R. Singh, S. Singh, P. Parihar, V. P. Singh and S. M. Prasad, *Ecotoxicol. Environ. Saf.*, 2015, **112**, 247–270.
261 A. K. Ghosh, P. Bhattacharyya and R. Pal, *Environ. Int.*, 2004, **30**, 491–499.
262 Y. K. Vishwakarma, S. Tiwari, D. Mohan and R. S. Singh, *Clean. Eng. Technol.*, 2021, **3**, 100115.
263 G. Chen, H. Shi, J. Tao, L. Chen, Y. Liu, G. Lei, X. Liu and J. P. Smol, *Sci. Rep.*, 2015, **5**, 1–7.
264 H. F. Bakhat, Z. Zia, S. Fahad, S. Abbas, H. M. Hammad, A. N. Shahzad, F. Abbas, H. Alharby and M. Shahid, *Environ. Sci. Pollut. Res.*, 2017, **24**, 9142–9158.
265 P. Colbourn, B. J. Alloway and I. Thornton, *Sci. Total Environ.*, 1975, **4**, 359–363.
266 Z. Q. Li, J. C. Yang, K. W. Sui and N. Yin, *Mater. Lett.*, 2015, **160**, 412–414.
267 J. B. Huo, L. Xu, J. C. E. Yang, H. J. Cui, B. Yuan and M. L. Fu, *Colloids Surf., A*, 2018, **539**, 59–68.
268 J. Sun, X. Zhang, A. Zhang and C. Liao, *J. Environ. Sci.*, 2019, **80**, 197–207.
269 Z. Li, X. Liu, W. Jin, Q. Hu and Y. Zhao, *J. Colloid Interface Sci.*, 2019, **554**, 692–704.

270 W. Yu, M. Luo, Y. Yang, H. Wu, W. Huang, K. Zeng and F. Luo, *J. Solid State Chem.*, 2019, **269**, 264–270.
271 P. Zhao, M. Jian, R. Xu, Q. Zhang, C. Xiang, R. Liu, X. Zhang and H. Liu, *Environ. Sci.: Nano*, 2020, **7**, 3616–3626.
272 Z. Liu, C. Wang, Y. Wu, L. Geng, X. Zhang, D. Zhang, H. Hu, Y. Zhang, X. Li, W. Liu and P. Na, *Polyhedron*, 2021, **196**, 114980.
273 B. Yang, X. Zhou, Y. Chen, Y. Fang and H. Luo, *Colloids Surf., A*, 2021, **629**, 127378.
274 T. Song, X. Feng, C. Bao, Q. Lai, Z. Li, W. Tang, Z. W. Shao, Z. Zhang, Z. Dai and C. Liu, *Sep. Purif. Technol.*, 2022, **288**, 120700.
275 M. N. Pervez, C. Chen, Z. Li, V. Naddeo and Y. Zhao, *Chemosphere*, 2022, **303**, 134934.
276 P. Kalimuthu, Y. Kim, M. P. Subbaiah, D. Kim, B. H. Jeon and J. Jung, *Chemosphere*, 2022, **294**, 133672.
277 W. Li, Z. Liu, L. Wang, G. Gao, H. Xu, W. Huang, N. Yan, H. Wang and Z. Qu, *J. Hazard. Mater.*, 2023, **446**, 130681.
278 W. Li, W. Ji, M. Yılmaz, T. C. Zhang and S. Yuan, *Appl. Surf. Sci.*, 2023, **609**, 155304.
279 X. He, F. Deng, T. Shen, L. Yang, D. Chen, J. Luo, X. Luo, X. Min and F. Wang, *J. Colloid Interface Sci.*, 2019, **539**, 223–234.
280 G. P. Gallios, A. K. Tolkou, I. A. Katsoyiannis, K. Stefusova, M. Vaclavikova and E. A. Deliyanni, *Sustainability*, 2017, **9**, 1684.
281 F. M. Jais, S. Ibrahim, Y. Yoon and M. Jang, *Sep. Purif. Technol.*, 2016, **169**, 93–102.
282 A. F. Hassan, A. M. Abdel-Mohsen and H. Elhadidy, *Int. J. Biol. Macromol.*, 2014, **68**, 125–130.
283 E. K. Jeon, S. Ryu, S. W. Park, L. Wang, D. C. W. Tsang and K. Baek, *J. Cleaner Prod.*, 2018, **176**, 54–62.
284 S. Kong, Y. Wang, Q. Hu and A. K. Olusegun, *Colloids Surf., A*, 2014, **457**, 220–227.
285 C. Wang, X. Liu, J. P. Chen and K. Li, *Sci. Rep.*, 2015, **5**, 1–10.
286 J. Li, Y. N. Wu, Z. Li, B. Zhang, M. Zhu, X. Hu, Y. Zhang and F. Li, *J. Phys. Chem. C*, 2014, **118**, 27382–27387.
287 M. Massoudinejad, M. Ghaderpoori, A. Shahsavani, A. Jafari, B. Kamarehie, A. Ghaderpoury and M. M. Amini, *J. Mol. Liq.*, 2018, **255**, 263–268.
288 Y. Gu, D. Xie, Y. Wang, W. Qin, H. Zhang, G. Wang, Y. Zhang and H. Zhao, *Chem. Eng. J.*, 2019, **357**, 579–588.
289 J. Sun, X. Zhang, A. Zhang and C. Liao, *J. Environ. Sci.*, 2019, **80**, 197–207.
290 M. Jian, H. Wang, R. Liu, J. Qu, H. Wang and X. Zhang, *Environ. Sci.: Nano*, 2016, **3**, 1186–1194.
291 X. Li, C. Wang, X. Chen, D. Li and Q. Jin, *J. Environ. Chem. Eng.*, 2023, **11**, 109038.
292 M. K. Ubhi, M. Kaur, D. Singh and V. K. Sharma, *J. Water Proc. engineering*, 2023, **52**, 103539.
293 L. I. M. Ayala, F. Aparicio, V. Boffa, G. Magnacca, L. Carlos, G. N. Bosio and D. O. Mártire, *Photochem. Photobiol. Sci.*, 2023, **22**, 503–512.
294 E. M. Opiso, C. B. Tabelin, L. M. Ramos, L. J. R. Gabiana, M. H. T. Banda, J. R. Y. Delfinado, A. H. Orbecido, J. B. Zoleta, I. Park, T. Arima and M. Villacorte-Tabelin, *J. Environ. Chem. Eng.*, 2023, **11**, 108992.
295 K. Folens, K. Leus, N. R. Nicomel, M. Meledina, S. Turner, G. Van Tendeloo, G. Du Laing and P. Van Der Voort, *Eur. J. Inorg. Chem.*, 2016, **2016**, 4395–4401.
296 J. Sun, X. Zhang, A. Zhang and C. Liao, *J. Environ. Sci.*, 2019, **80**, 197–207.
297 F. Zahir, S. J. Rizwi, S. K. Haq and R. H. Khan, *Environ. Toxicol. Pharmacol.*, 2005, **20**, 351–360.
298 R. Kumar Verma, M. Singh Sankhla and R. Kumar, *International Journal of Forensic Science*, 2018, **1**, 72–78.
299 H. M. Abd El Salam and T. Zaki, *Egypt. J. Chem.*, 2019, **62**, 837–851.
300 Y. Y. Xiong, J. Q. Li, L. Le Gong, X. F. Feng, L. N. Meng, L. Zhang, P. P. Meng, M. B. Luo and F. Luo, *J. Solid State Chem.*, 2017, **246**, 16–22.
301 Z. Zhang, J. Liu, Z. Wang and Y. Yang, *Fuel*, 2021, **289**, 119791.
302 T. Liu, J. X. Che, Y. Z. Hu, X. W. Dong, X. Y. Liu and C. M. Che, *Chem. –A Euro. J.*, 2014, **20**, 14090–14095.
303 P. Yang, Y. Shu, Q. Zhuang, Y. Li and J. Gu, *Chem. Commun.*, 2019, **55**, 12972–12975.
304 K. Leus, J. P. H. Perez, K. Folens, M. Meledina, G. Van Tendeloo, G. Du Laing and P. Van Der Voort, *Faraday Discuss.*, 2017, **201**, 145–161.
305 A. Esrafili, M. Ghambarian, M. Tajik and M. Baharfar, *Anal. Methods*, 2020, **12**, 2279–2286.
306 K. Xia, Y. Guo, Q. Shao, Q. Zan and R. Bai, *Nanomaterials*, 2019, **9**, 1532.
307 A. Srikhaow, T. Butburee, W. Pon-On, T. Srikhirin, K. Uraisin, K. Suttiponpanit, S. Chaveanghong and S. M. Smith, *Appl. Sci.*, 2020, **10**, 8262.
308 M. Naushad, T. Ahamad, Z. A.-J. and A. H. Al-Muhtaseb, 2019, Green and eco-friendly nanocomposite for the removal of toxic Hg (II) metal ion from aqueous environment: adsorption kinetics & isotherm modelling, Elsevier.
309 K. Ghanemi, M. Badri, K. Hardani, F. Buazar, K. Ghanemi, M. Kashisaz, M. H. Baghlani-Nezhad, A. Khaledi-Naseb and M. Badri, *AASCIT J. Nanosci.*, 2015, **1**, 11–18.
310 Y. Zhao, K. Xia, Z. Zhang, Z. Zhu, Y. Guo and Z. Qu, *Nanomaterials*, 2019, **9**, 455.
311 P. Yang, Y. Shu, Q. Zhuang, Y. Li and J. Gu, *Chem. Commun.*, 2019, **55**, 12972–12975.
312 G. P. Li, K. Zhang, P. F. Zhang, W. N. Liu, W. Q. Tong, L. Hou and Y. Y. Wang, *Inorg. Chem.*, 2019, **58**, 3409–3415.
313 Y. He, Y. L. Hou, Y. L. Wong, R. Xiao, M. Q. Li, Z. Hao, J. Huang, L. Wang, M. Zeller, J. He and Z. Xu, *J. Mater. Chem. A*, 2018, **6**, 1648–1654.
314 Y. Wu, G. Xu, F. Wei, Q. Song, T. Tang, X. Wang and Q. Hu, *Microporous Mesoporous Mater.*, 2016, **235**, 204–210.
315 H. Saleem, U. Rafique and R. P. Davies, *Microporous Mesoporous Mater.*, 2016, **221**, 238–244.
316 Z. Q. Li, J. C. Yang, K. W. Sui and N. Yin, *Mater. Lett.*, 2015, **160**, 412–414.
317 E. Hatzidaki, G. N. Tzanakakis and A. M. Tsatsakis, *Med Sci Monit*, 2005, **11**(10), 329–336.
318 A. L. Wani, A. Ara and J. A. Usmani, *Interdiscip. Toxicol.*, 2015, **8**, 55–64.

319 M. C. Nagar, M. L. Dotaniya, A. Sharma, C. K. Dotaniya, R. K. Doutaniya and J. K. Saha, *Environ. Monit. Assess.*, 2023, **195**, 1–9.
320 N. Yin, K. Wang, L. Wang and Z. Li, *Chem. Eng. J.*, 2016, **306**, 619–628.
321 N. David Shooto, D. Wankasi, L. Sikhwivhilu and D. Dikio, *Asian J. Chem.*, 2018, **28**, 277–281.
322 Z. Shi, C. Xu, H. Guan, L. Li, L. Fan, Y. Wang, L. Liu, Q. Meng and R. Zhang, *Colloids Surf., A*, 2018, **539**, 382–390.
323 K. Wang, J. Gu and N. Yin, *Ind. Eng. Chem. Res.*, 2017, **56**, 1880–1887.
324 Y. Zhang, H. Zheng, P. Zhang, X. Zheng and Q. Zuo, *J. Hazard. Mater.*, 2021, **408**, 124917.
325 A. M. Ghaedi, M. Panahimehr, A. R. S. Nejad, S. J. Hosseini, A. Vafaei and M. M. Baneshi, *J. Mol. Liq.*, 2018, **272**, 15–26.
326 P. Goyal, C. S. Tiwary and S. K. Misra, *J. Environ. Manage.*, 2021, **277**, 111469.
327 H. Zhu, J. Yuan, X. Tan, W. Zhang, M. Fang and X. Wang, *Environ. Sci.: Nano*, 2019, **6**, 261–272.
328 N. Abdollahi, S. A. Akbar Razavi, A. Morsali and M. L. Hu, *J. Hazard. Mater.*, 2020, **387**, 121667.
329 I. Ijaz, A. Bukhari, E. Gilani, A. Nazir and H. Zain, *RSC Adv.*, 2023, **13**, 5643–5655.
330 C. Yu, Z. Shao and H. Hou, *Chem. Sci.*, 2017, **8**, 7611–7619.
331 B. F. M. L. Gomes, C. M. B. de Araújo, B. F. do Nascimento, E. M. P. L. de Freire, M. A. Da Motta Sobrinho and M. N. Carvalho, *Environ. Sci. Pollut. Res.*, 2022, **29**, 17358–17372.
332 J. Anwar, U. Shafique, Waheed-uz-Zaman, M. Salman, A. Dar and S. Anwar, *Bioresour. Technol.*, 2010, **101**, 1752–1755.
333 L. P. Lingamdinne, O. Amelirad, J. R. Koduru, R. R. Karri, Y. Y. Chang, M. H. Dehghani and N. M. Mubarak, *J. Water Process Eng.*, 2023, **51**, 103386.
334 S. Sepehri, E. Kanani, S. Abdoli, V. D. Rajput, T. Minkina and B. Asgari Lajayer, *Water*, 2023, **15**, 222.
335 J. Li, Z. Hu, Y. Chen and R. Deng, *Water*, 2023, **15**, 1857.
336 K. Tang, S. Zhang, D. Ren, X. Zhang, Z. Zhang and X. Zhang, *Water Sci. Technol.*, 2023, **87**, 1096–1111.
337 Z. Hao, D. Nie, M. Zhang, W. Wang, D. Zou and G. Nie, *Chem. Eng. J.*, 2023, **465**, 142721.
338 G. Zhou, S. Li, C. Niu, Q. Wang, X. Zhang, Q. Meng and L. Li, *Environ. Sci. Pollut. Res.*, 2023, **30**, 39169–39183.
339 H. Zhu, J. Yuan, X. Tan, W. Zhang, M. Fang and X. Wang, *Environ. Sci.: Nano*, 2019, **6**, 261–272.
340 A. Hakimifar and A. Morsali, *Inorg. Chem.*, 2019, **58**, 180–187.
341 A. M. Ghaedi, M. Panahimehr, A. R. S. Nejad, S. J. Hosseini, A. Vafaei and M. M. Baneshi, *J. Mol. Liq.*, 2018, **272**, 15–26.
342 R. Ricco, K. Konstas, M. J. Styles, J. J. Richardson, R. Babarao, K. Suzuki, P. Scopece and P. Falcaro, *J. Mater. Chem. A*, 2015, **3**, 19822–19831.
343 Y. Song, N. Wang, L. Y. Yang, Y. G. Wang, D. Yu and X. K. Ouyang, *Ind. Eng. Chem. Res.*, 2019, **58**, 6394–6401.
344 H. Saleem, U. Rafique and R. P. Davies, *Microporous Mesoporous Mater.*, 2016, **221**, 238–244.
345 F. Zhao, C. Su, W. Yang, Y. Han, X. Luo, C. Li, W. Tang, T. Yue and Z. Li, *Appl. Surf. Sci.*, 2020, **527**, 146862.
346 A. Zhitkovich, *Chem. Res. Toxicol.*, 2011, **24**, 1617–1629.
347 K. Shekhawat, S. Chatterjee and B. Joshi, *Int. J. Adv. Res.*, 2015, **3**(7), 167–172.
348 M. N. Georgaki and M. Charalambous, *J. Water Health*, 2023, **21**, 205–223.
349 M. E. Mahmoud, S. M. Elsayed, S. M. E. Mahmoud, R. O. Aljedaani and M. A. Salam, *J. Mol. Liq.*, 2022, **347**, 118274.
350 Z. Hasan, J. Cho, J. Rinklebe, Y. S. Ok, D. W. Cho and H. Song, *J. Ind. Eng. Chem.*, 2017, **52**, 331–337.
351 Z. Lv, X. Tan, C. Wang, A. Alsaedi, T. Hayat and C. Chen, *Chem. Eng. J.*, 2020, **389**, 123428.
352 H. Fu, L. Wu, J. Hang, P. Wang, C. Zhao and C. C. Wang, *J. Alloys Compd.*, 2020, **837**, 155567.
353 Y. Qing, W. Gao, Y. Long, Y. Kang and C. Xu, *Inorg. Chem.*, 2023, **62**, 6909–6919.
354 D. Yuan, C. Shang, J. Cui, W. Zhang and Y. Kou, *Environ. Res.*, 2023, **216**, 114616.
355 M. Tan, H. Du, Y. Fu, X. Ma, N. Li, D. Hao and Q. Wang, *Int. J. Hydrogen Energy*, 2023, **48**, 18719–18730.
356 L. Yang, X. Liu, T. Yang, Z. Chen, J. Guo, L. Zheng, X. Xiao, G. Zeng, X. Luo and S. Luo, *Resour., Conserv. Recycl.*, 2023, **191**, 106884.
357 Y. Fang, J. Wen, H. Zhang, Q. Wang and X. Hu, *Environ. Pollut.*, 2020, **260**, 114021.
358 A. Rahman, M. A. Haque, S. Ghosh, P. Shinu, M. Attimarad and G. Kobayashi, *Sustainability*, 2023, **15**, 2431.
359 S. Ehsanpour, M. Riahi Samani and D. Toghraie, *Alexandria Eng. J.*, 2023, **64**, 581–589.
360 E. M. Chatir, A. El Hadrami, S. Ojala, G. El Mouhri and R. Brahmi, *Int. J. Environ. Anal. Chem.*, 2023, DOI: **10.1080/03067319.2023.2177956**.
361 J. Garvasis, A. R. Prasad, K. O. Shamsheera, T. A. Nidheesh Roy and A. Joseph, *Mater. Res. Bull.*, 2023, **160**, 112130.
362 Y. Bin, Q. Liang, H. Luo, Y. Chen and T. Wang, *Environ. Sci. Pollut. Res.*, 2023, **30**, 6746–6757.
363 Q. Wang, W. Zuo, Y. Tian, L. Kong, G. Cai, H. Zhang, L. Li and J. Zhang, *Chemosphere*, 2023, **329**, 138622.
364 Y. Chen, J. Yang and A. Abbas, *Toxics*, 2023, **11**, 440.
365 G. Gao, L. Nie, S. Yang, P. Jin, R. Chen, D. Ding, X. C. Wang, W. Wang, K. Wu and Q. Zhang, *Appl. Surf. Sci.*, 2018, **457**, 1208–1217.
366 D. T. C. Nguyen, H. T. N. Le, T. Van Tran, O. T. K. Nguyen, T. D. Nguyen, D. T. Sy, D. V. N. Vo, T. D. Lam, L. G. Bach and D. Van Thuan, *Mater. Today: Proc.*, 2019, **18**, 2422–2429.
367 H. Hu, J. Liu, Z. Xu, L. Zhang, B. Cheng and W. Ho, *Appl. Surf. Sci.*, 2019, **478**, 981–990.
368 L. Aboutorabi, A. Morsali, E. Tahmasebi and O. Büyükgüngor, *Inorg. Chem.*, 2016, **55**, 5507–5513.
369 H. R. Fu, Z. X. Xu and J. Zhang, *Chem. Mater.*, 2015, **27**, 205–210.
370 A. Nasrollahpour and S. E. Moradi, *Microporous Mesoporous Mater.*, 2017, **243**, 47–55.
371 S. Rapti, A. Pournara, D. Sarma, I. T. Papadas, G. S. Armatas, Y. S. Hassan, M. H. Alkordi,

M. G. Kanatzidis and M. J. Manos, *Inorg. Chem. Front.*, 2016, **3**, 635–644.
372 E. Tahmasebi, M. Y. Masoomi, Y. Yamini and A. Morsali, *Inorg. Chem.*, 2015, **54**, 425–433.
373 Z. Xie, S. Diao, R. Xu, G. Wei, J. Wen, G. Hu, T. Tang, L. Jiang, X. Li, M. Li and H. Huang, *Appl. Surf. Sci.*, 2023, **636**, 157827.
374 R. Soltani, R. Pelalak, M. Pishnamazi, A. Marjani and S. Shirazian, *Arabian J. Chem.*, 2021, **14**, 103052.
375 J. Li, G. Lin, Z. Zhong, Z. Wang, S. Wang, L. Fu and T. Hu, *Int. J. Biol. Macromol.*, 2024, **258**, 129170.
376 P. Chen, Y. Wang, X. Zhuang, H. Liu, G. Liu and W. Lv, *J. Environ. Sci.*, 2023, **124**, 268–280.
377 Z. A. Al-Ahmed, M. Alhasani, M. M. Aljohani, R. M. Snari, H. A. Alghasham, N. M. Alatawi, A. A. Keshk and N. M. El-Metwaly, *Int. J. Biol. Macromol.*, 2024, **259**, 129282.
378 H. M. Nassef, G. A. A. M. Al-Hazmi, A. A. A. Alayyafi, M. G. El-Desouky and A. A. El-Bindary, *J. Mol. Liq.*, 2024, **394**, 123741.
379 S. W. Lv, J. M. Liu, C. Y. Li, N. Zhao, Z. H. Wang and S. Wang, *Chem. Eng. J.*, 2019, **375**, 122111.
380 C. Ji, M. Xu, H. Yu, L. Lv and W. Zhang, *J. Hazard. Mater.*, 2022, **424**, 127684.
381 T. Wu, J. Lei, L. Lin, Q. Wang, T. H. Farooq, G. Wang, J. Wang and W. Yan, *Environ. Technol. Innovation*, 2023, **32**, 103428.
382 M. N. Nimbalkar and B. R. Bhat, *J. Environ. Chem. Eng.*, 2021, **9**, 106216.
383 N. M. Mahmoodi, M. Taghizadeh, A. Taghizadeh, J. Abdi, B. Hayati and A. A. Shekarchi, *Appl. Surf. Sci.*, 2019, **480**, 288–299.
384 Z. Guo, J. Zhou, H. Hou, X. Wu and Y. Li, *J. Solid State Chem.*, 2023, **323**, 124059.
385 W. Ji, W. Li, Y. Wang, T. C. Zhang and S. Yuan, *Sep. Purif. Technol.*, 2024, **334**, 126003.